

## ABSTRACT

ARULALAN, KARTHIK SURESH, *C. elegans* Stress Response to Xenobiotic Mixtures under different Environmental Conditions using Mixture DoE Approach. (Under the direction of Dr. Adriana San Miguel Delgadillo).

Pollutant mixtures are complicated in nature. It is necessary to understand the mechanism of toxicity of such mixtures using *in vivo* models as they have been implicated in human disease progression. Environmental conditions also play an important role in determining the toxicity mechanism as well as the response mounted by *in vivo* models to such mixtures. 1,4-Naphthoquinones are a family of compounds exerting oxidative stress through different mechanisms. Oxidative stress has been observed in organisms used to study neurodegenerative diseases, however the source of stress has not been clearly understood. *C. elegans* model with fluorescent tagged *gst-4* gene can be used to study oxidative stress response to external compounds. The dynamic response mounted by organisms to xenobiotics mixtures under different environmental conditions is used to study the oxidative stress mechanisms of naphthoquinone mixtures. It was observed that individual compounds elicited a higher response compared to the binary and ternary mixtures under no accompanying environmental stress conditions. Dietary restriction had a synergistic effect with oxidative stress response to juglone and the mixtures. Simultaneous heat stress attenuated the *gst-4* response to the mixtures under both *ad libitum* and dietary restriction. These results indicate that the response mounted by *C. elegans* to naphthoquinone mixtures under different environmental conditions is driven by multiple pathways parallelly. Further studies with biomarkers for heat stress response and dietary restriction can help us understand the complexity of response mounted by *C. elegans* at different time points.

© Copyright 2020 by Karthik Suresh Arulalan

All Rights Reserved

*C. elegans* Stress Response to Xenobiotic Mixtures under different Environmental Conditions  
using Mixture DoE Approach.

by  
Karthik Suresh Arulalan

A thesis submitted to the Graduate Faculty of  
North Carolina State University  
in partial fulfillment of the  
requirements for the degree of  
Master of Science

Chemical Engineering

Raleigh, North Carolina  
2020

APPROVED BY:

---

Adriana San Miguel Delgadillo  
Committee Chair

---

Jonathan Stallrich

---

Qingshan Wei

## **BIOGRAPHY**

Karthik Suresh Arulalan was born and raised in Chennai, Tamil Nadu, India. He received his B.Tech in Chemical Engineering from Alagappa College of Technology Campus, Anna University in 2018. In 2018, he joined North Carolina State University to pursue graduate studies in Chemical Engineering. He joined Dr. San Miguel's lab in December 2018 as a research assistant. He investigated the use of Design of experiment methodology for studying oxidative stress response of *C. elegans*.

## ACKNOWLEDGMENTS

First and foremost, I would like to express my gratitude to my advisor Dr. Adriana San Miguel for taking me into her lab and trusting me to pursue my thesis. Her encouragement and enthusiasm allowed me to apply ideas I learnt in graduate classes in my thesis project.

I am grateful to Javier Huayta for helping me in my project and teaching valuable lab skills. I would also like to thank other members of the group, Danny, Sahand, Rita, Andrew, James and Joshua for helping me achieve my goals in the lab. I would also like to thank Dr. Stallrich for his patient support and inputs helping me understand the fundamentals of Statistics and JMP.

I would like to thank Sahand, Javier, Danny, Ryan, Tommy, Chris, Rakshit, Eduardo, Zack, Vernon, Sudeep, Vikram, Sanjai for making the stay at North Carolina State University a pleasant and memorable one. I would like to thank my grandmother S.D. Baghyam and mother M.B.Parameswari for being role models and supporting me in this journey. I also extend my thanks to my father, brother, and other friends.

**TABLE OF CONTENTS**

LIST OF TABLES .....	vi
LIST OF FIGURES .....	vii
CHAPTER 1: INTRODUCTION .....	1
CHAPTER 2: LITERATURE REVIEW .....	3
2.1 Oxidative stress and relevance to disease models.....	3
2.2 Xenobiotic oxidative stressors .....	4
2.3 Effect of xenobiotic mixtures.....	4
2.4 Cytotoxic activity of 1,4-Naphthoquinones .....	5
2.5 <i>C. elegans</i> as a model organism.....	7
2.6 Oxidative stress response of <i>C. elegans</i> .....	8
2.7 Effect of environmental factors on oxidative stress response.....	10
2.8 <i>gst-4</i> as a biomarker of SKN-1 pathway.....	11
2.9 Design of Experiments (DoE) approach.....	12
2.10 Mixture model and optimal design .....	13
2.11 Optimal design generation in JMP.....	17
CHAPTER 3: MATERIALS AND METHODS .....	18
3.1 Strain maintenance.....	18
3.2 Chemical preparation .....	18
3.3 Design generation .....	19
3.4 Application of oxidative stress and fluorescent imaging .....	20
3.5 Quantitative image processing.....	21
3.6 Statistical analysis.....	21

CHAPTER 4: RESULTS AND DISCUSSION.....	23
4.1 Dose dependency .....	23
4.2 1,4-Naphthoquinone mixtures under fixed process conditions.....	25
4.3 1,4-Naphthoquinone mixtures under changing process conditions .....	27
4.4 Discussion.....	33
CHAPTER 5: CONCLUSION AND FUTURE DIRECTIONS .....	37
5.1 Conclusion .....	37
5.2 Future directions .....	37
REFERENCES .....	40

**LIST OF TABLES**

Table 4.1. Effect of experimental treatment application process on the first experiment.....	26
Table 4.2. Testing for significant effects in first mixture experiment.....	27
Table 4.3. Effect of experimental treatment application process on the second experiment. ...	30
Table 4.4. Testing for significant effects in second mixture experiment. ....	32

## LIST OF FIGURES

Figure 2.1. a. 1,4-naphthoquinone b. Juglone c. Plumbagin.....	7
Figure 2.2. Toxicity mechanism of Naphthoquinones. a. Redox cycling b. Michael’s addition. SOD Superoxide dismutase. GPx Glutathione peroxidase. GSH- Glutathione GSSG – Glutathione disulphide. ....	8
Figure 2.3. Simplex lattice design for a first order Scheffé model is a “slice” of the response space since the sum of the components is fixed. ....	15
Figure 2.4. a. Simplex lattice design for a second order Scheffé model b. Simplex centroid design for special Scheffé model.....	16
Figure 3.1. Image Processing methodology a. Unprocessed image. b. Binary mask c. Overlap of mask onto the image to quantify intensity.....	22
Figure 4.1. Dose dependent <i>gst-4</i> response to individual compounds.....	23
Figure 4.2. Control chart of the 10 populations used to perform the first mixture experiment. .	26
Figure 4.3. Response surface of first mixture response .....	27
Figure 4.4. Testing for main effects of process variables .....	29
Figure 4.5. Control chart of 28 populations used to perform the second mixture experiment ...	31
Figure 4.6. Effect of process variables on the oxidative stress response to 1,4-Naphthoquinone mixtures .....	31

## CHAPTER 1 INTRODUCTION

A large amount of literature is dedicated toward understanding the mechanisms of toxicity of individual compounds classified as environmental pollutants[1]–[4]. However, pollutants are present in the form of mixtures in the environment pollutants [1]–[4](Carpenter, 1998) (Backhaus, 2012) (Braun, 2016) (Carvalho, 2004). The Environmental Protection Agency (EPA) has proposed simple additive models to define the toxicity of the mixtures [5]. Studies have shown that such toxic pollutant mixtures have synergistic and antagonistic effects on both *in vitro* and *in vivo* models [4]–[6]. This highlights the importance of studying the mechanism of toxicity caused by such mixtures. Additionally, environmental factors are also suspected to play an important role in the chronic toxicity caused by pollutant compounds which can lead to significant role in disease advancement [7]. It is pertinent to study the risks posed by such toxic mixtures and their interaction with environmental factors in human disease progression [7]. 1,4-Naphthoquinones are a class of compounds usually used as precursors for industrially relevant compounds such as anthraquinone, dithianon and are toxic in nature [8]. The cytotoxicity and genotoxicity of the individual 1,4-Naphthoquinones compounds have been studied extensively [9]. The compounds have been hypothesized to induce oxidative stress through two distinct mechanisms [10]. It is necessary to study different factors which play a role in increasing oxidative stress as it is observed while studying neurodegenerative diseases in model organisms [11]–[13]. The compounding effects of oxidative stress induced by naphthoquinone mixtures in different environmental conditions can help us understand the toxicity of mixtures.

*C. elegans* has proven to be a good model organism to study the oxidative stress response due to its small size, easy maintenance, mapped genome and ability to perform *in vivo* studies using fluorescent markers due to their transparent bodies [14]. They are also used a models to

study neurodegenerative disease progression under the influence of genetic and environmental factors [15]. Previous studies on growth and fertility of *C. elegans* in the presence of fungicides, and heavy metal mixtures have proven that they are good models to study mixture toxicity [16]–[20]. In *C. elegans*, the oxidative stress response pathway, cascade is activated to reduce the toxicity caused by oxidative stressors [21]. The response mounted by *C. elegans* is evolutionarily conserved up to mammalian cells thus cementing their status to be used as model organisms to study mixtures.

Design of Experiments is an approach where the input factors in experiments are systematically varied in a particular order to determine their influence [22]. In a mixture experimental design, the main effects are the different proportions of the components in a mixture. This is achieved by placing a constraint on total amount of mixture [23]. We can prevent wrongful interpretation of the mixture experiment as the constraint would allow us to test for significant mixture proportions without potential confounding with total amount of mixture [23]. Thus, standard, and optimized mixture designs can be used to study the impact of mixtures proportions under different process conditions.

In this study, the oxidative stress response mounted by *C. elegans* in response to 1,4-naphthoquinone mixtures have been studied. Standard mixture designs were used to analyze the mixture proportions. The response of the worms to the mixtures was observed using a strain with green fluorescent protein tagged to *gst-4* gene, a proxy for SKN-1 activity during oxidative stress response. Differential responses by the organism to the individual naphthoquinones and mixtures were observed at the different environmental conditions.

## CHAPTER 2 LITERATURE REVIEW

### 2.1 Oxidative stress and relevance to disease models

Oxidative stress occurs when there is an imbalance between formation and depletion of the Reactive Oxygen Species (ROS) in cells and tissues [24]. Since molecular oxygen cannot react with most biomolecules, there is an addition of a single electron to oxygen generating ROS - superoxide, hydrogen peroxide ( $H_2O_2$ ), the hydroxyl radical ( $OH\cdot$ ), and water. The primary generators of ROS are mitochondria during physiological conditions [25]. ROS are constantly produced as a product of enzymatic and non-enzymatic reactions. ROS are necessary since they are involved in cell signaling and physiology [24]. For example,  $H_2O_2$  has been shown to potentiate ASH neuron involved in the avoidance behavior seen in the *C. elegans* worm model [26]. NADPH oxidase and dual oxidase family of enzymes reduce  $O_2$  to  $O_2\cdot^-$  in phagocytic cells present in mammals [27]. However, ROS can be externally generated due to environmental stressors such as UV light, ionizing radiations, pollutants, heavy metals and cytotoxins [20], [28], [29]. The excess free radicals and oxidants can affect membranes, lipids, proteins, lipoproteins, and DNA. Such irreversible damage can manifest as diseases at the organism level. Multiple studies implicate oxidative stress in neurodegenerative disease's mechanism of causation [13], [30]. Detailed reviews of the role of oxidative stress in AD, PD can be found in Huang et al. and Dias et al respectively [13], [30]. Neurodegenerative diseases such as Huntington's disease (HD), Alzheimer's disease (AD) and Parkinson's disease (PD) are projected to increase in the global population [30], [31]. For example, Huntington's disease has been known to affect 1 in 7500 individuals in a global population, and this number is expected to increase in the next century [31]. It is pertinent to identify the role of environmental agents for increase in oxidative stress in organisms to tackle such diseases.

## 2.2 Xenobiotic oxidative stressors

Compounds that are “foreign” to the organism of interest including environmental pollutants, metal ions, drugs, and phytochemicals elicit responses ranging from changes in cell signaling, adaptation, and initiation of cell death. Xenobiotic oxidative stress is induced when excess generation of ROS species is caused by compounds of differing chemical nature such as paraquat, acrylamide, H<sub>2</sub>O<sub>2</sub>, juglone [32]–[34]. For example, paraquat is a quaternary nitrogen compound widely used as a herbicide. It is a swift, non-selective compound, which causes damage to plant tissue through physical contact. It is present in the environment as pollutant after excessive use [35]. It exerts its herbicide activity by obstructing the intracellular electron transfer systems in plants, thereby inhibiting reduction of NADP to NADPH during photosynthesis [36]. This disruption leads to the formation of superoxide anion, singlet oxygen, as well as hydroxyl and peroxy radicals that affect cellular components. Paraquat has been observed to elicit toxicity in other organisms including humans. A detailed mechanism of toxicity treatment for paraquat poisoning in humans is given by Oliveira et al. [37]. The other compounds mentioned are also considered as toxic in nature due to the oxidative stress exerted by them [33], [34].

## 2.3 Effect of xenobiotic mixtures

Industrialization, despite its immense contribution to the world has resulted in the increase of pollutants which are present in the form of mixtures. Mechanism of toxicity is usually studied at a single compound level. Pollutant mixtures are complex in nature even if the individual compounds are present at concentrations well below the safety limit as defined by the regulations [4]. As mentioned in the introduction, the US EPA has defined dose additivity for compounds having similar mechanisms of action and response additivity for compounds with different mechanisms [5]. Recent studies have been performed to study the toxicity of these mixtures using

different cell models and model organisms. Parvez et al. used the *Vibrio fischeri* bioluminescence assay to study the impact of pollutants from different industries as defined by US EPA toxicity release inventory database [38]. Feng et al. used *C. elegans* model organisms to study time dependent toxicity of mixtures containing common and emerging pollutants [6]. They observed that while mixture exhibited synergistic toxic effects initially, the synergistic effects decreased with time. Tang et al. studied the toxic effect of Cd, Mn and Pb metal mixtures on *C. elegans* body length, brood size and feeding. They observed that binary mixtures of Cd and Mn showed antagonistic effects than individual metals, while other binary mixtures and ternary mixtures had synergistic effects. Moser et al. studied neurobehavioral degeneration in rat models commonly occurring pollutant mixtures in superfund sites [5]. Mixtures of trichloroethylene (TCE), di(2-ethylhexyl) phthalate (DEHP), and heptachlor (HEPT) was fed to the rats and neuronal behavior was tracked using motor activity and collection of tests. Interestingly, the conservative assumption of additive and synergistic effects was observed for some observational parameters while few antagonistic effects were observed for other parameters. More studies are necessary to understand the mechanism of pollutant mixtures, models for predicting interactions and designs for analyzing mixtures.

#### **2.4 Cytotoxic activity of 1,4-Naphthoquinones**

Naphthoquinones are secondary metabolic cytotoxins produced in plants and products of fuel combustion, tobacco smoke [39], [40]. Compounds such as 1,4-Naphthoquinone, 5-Hydroxy-p-naphthoquinone (juglone), 5-hydroxy-2-methyl-1,4-naphthoquinone (plumbagin) shown in figure 2.1 belong to this family. They are also present as mixtures in the naturally occurring form [41]–[44]. The chemical structure of the monomeric naphthoquinones is based on the bicycle system - naphthalene skeleton with functional group substitution in C1 and C4 [39]. The

compounds have been shown to elucidate oxidative stress in *in vivo* models as well as mutagenic activity in *in vitro* studies [9]. Initially, it was hypothesized that the compounds of the naphthoquinone family had a singular mechanism to elicit oxidative stress [45]. The compounds have been proposed to elicit oxidative stress through 2 distinct mechanisms as shown in figure 2.2. They can cause depletion in glutathione activity, an important phase 2 detoxification enzyme [10]. They can also cause production of ROS species through redox cycling [10]. The initiation of ROS production in biological settings is dependent on the compound's ability to form free-radical metabolites [46]. The stability of these intermediates is known to decide the degree of cytotoxic activity. Studies have been performed under aqueous and aprotic conditions to mimic the stability and activity of the intermediates in biological cells [45], [46]. Electrochemical and spectroelectrochemical study revealed differences in reactivity of semiquinone radicals produced by plumbagin and juglone [46]. Plumbagin produced more stable radical anions, while those generated by the juglone are more reactive and undergo a self-protonation due to activity of the OH functional group. Inbaraj et al. observed differences in the cytotoxic mechanism of juglone and plumbagin based on studies on HaCaT Keratinocytes [10]. It was reported that plumbagin stoichiometrically converted glutathione (GSH) to glutathione disulphide (GSSG) by redox cycling while juglone is assumed to directly undergo nucleophilic addition to GSH. Hunt et al. studied the effect of different orthologs of naphthoquinones on the stress response and lifespan of *C. elegans*. Sublethal dose of plumbagin invoked SKN-1 dependent stress response while oxoline, menadione did not invoke a SKN-1 dependent stress response. The differences in cytotoxic mechanisms of 1,4-Naphthoquinones warrant us to use them as an illustration for understanding oxidative stress exerted by mixtures.

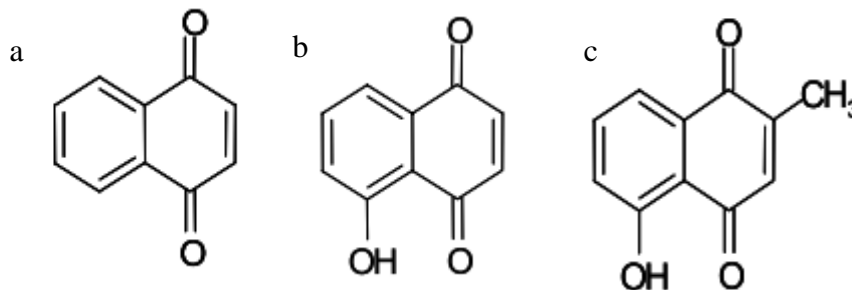


**Figure 2.1. a. 1,4-naphthoquinone b. Juglone c. Plumbagin**

## 2.5 *C. elegans* as a model organism

*C. elegans* is a microscopic organism found all around the world. The nematodes grow from 0.25 millimeters to adults that are 1 millimeter long. The worms are self-fertilizing hermaphrodites, with less than 0.2% developed males in a population enabling reproduction of isogenic populations [47]. The small size of the animal and its transparent body enables visualization of individual cells and subcellular features using confocal microscopy. Its genome can be engineered to add fluorescence tags to proteins or subcellular features to track their activity *in vivo*. *C. elegans* has a relatively short lifespan of 14-21 days that enables us to study age dependent change in features of interest [14]. *C. elegans* has proven to be a good *in vivo* model to study diseases because 40% of the genes associated with human disease have conserved orthologs in *C. elegans* genome [48]. The gene expression in the animal is studied using different methods such as microarrays, PCR, RT-PCR, RNA Sequencing and serial analysis of gene expression (SAGE) techniques [32], [49], [50]. These enable us to study genetic pathways under different conditions such as age, sex, developmental time, and environmental factors such as temperature, diet and presence of other chemicals. These techniques, however, require the worms to be killed in order to extract and isolate the RNA for analysis. The intense human labor required to carry out these elaborate protocols also are deemed disadvantageous. Due to advancement in genetic engineering, it is possible to generate transgenic *C. elegans* strain lines containing fluorophores

such as green fluorescent protein (GFP) tagged to specific proteins [51]. This allows us to surpass the disadvantages of the previous methods and allows high throughput in vivo analysis of the animals [52]

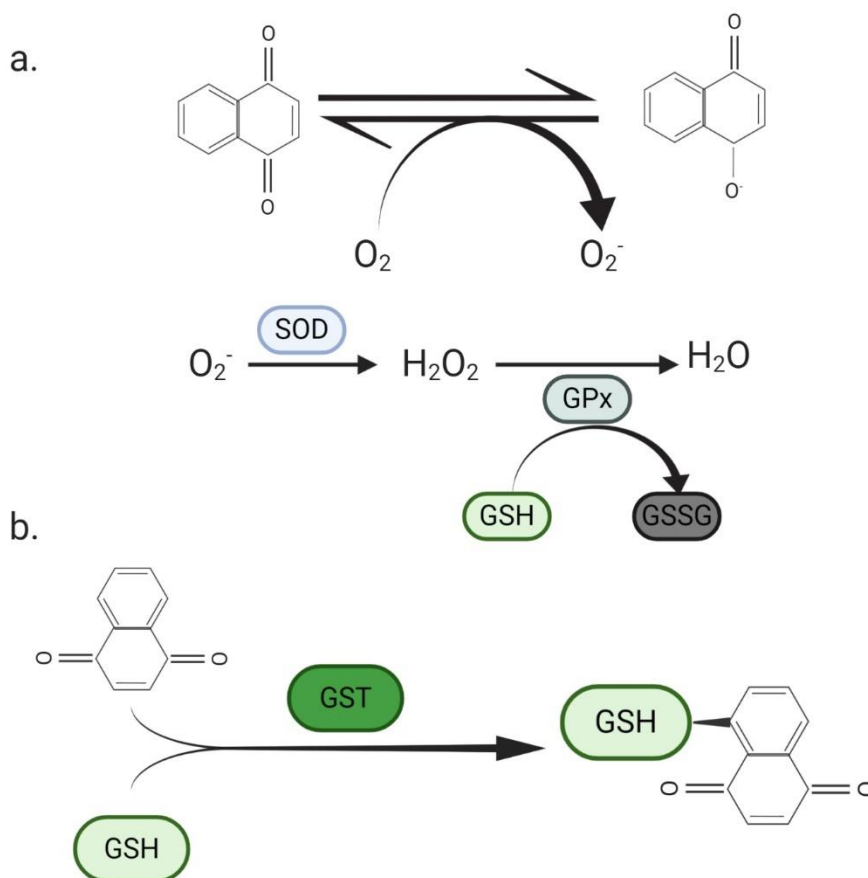


**Figure 2.2. Toxicity mechanism of Naphthoquinones. a. Redox cycling b. Michael's addition. SOD Superoxide dismutase. GPx – Glutathione peroxidase. GSH- Glutathione GSSG – Glutathione disulphide.**

## 2.6 Oxidative stress response of *C. elegans*

Cells of the organisms have defense mechanisms to deal with xenobiotics. They upregulate the genes responsible for transcribing proteins involved in the biotransformation of the xenobiotics to relatively less harmful and harmless byproducts. The defense mechanism usually occurs in three

stages. The first stage involves the detection and marking of the external compounds for coupling with proteins involved in the biotransformation. The second stage is the biotransformation to secondary metabolites. The third stage is then transportation and excretion of such metabolites. These defense mechanisms to metabolize and eliminate the xenobiotics are evolutionarily conserved from single cell organisms to mammalian human cells [53]. NRF-1, NRF-2, NRF-3 are a class of NF-E2-related factor 2 (NRF) transcription regulators in mammalian cells. They have a cap and collar domain and DNA binding region. The Nrf-2 transcription factor has a functional ortholog in *C. elegans*: SKN-1 [54]. It should be noted that SKN-1 diverges from Nrf-2 in the way it binds to DNA. However, the similarities allow us to study the SKN-1 in *C. elegans* as a model for mammalian NRF-2 [54]. Antioxidant Response Elements (ARE)-binding and ROS induced genes are present mostly in the intestine and are regulated by the SKN-1 pathway. SKN-1 has also been linked to other much broader homeostatic functions such as reducing stress, counteracting lipid accumulation, mitochondrial biogenesis and mitophagy, among others [54]. Under non-stress conditions, SKN-1 is only present in the cytoplasm of the cells. Under oxidative stress, SKN-1 translocation to the nucleus of intestine cells has been observed, where it can bind DNA and start expression of stress response genes [54]. The translocation to the nucleus is mediated by the conserved p38 MAP kinase signaling pathway [55]. The nuclear accumulation is counteracted by WDR-23 under normal circumstances [56]. Under oxidative stress, WDR-23 activity is reduced.

In *C. elegans*, SKN-1 activity is studied by examining downstream protein expression in the different tissues through fusion to fluorescent proteins as mentioned in the previous section. The response is extensively studied in the intestine where digestion and detoxification occur. Multiple ARE-containing genes are downstream targets of SKN-1, such as *gst-4* and *gcs-1*, each

encoding for drug-metabolizing glutathione S-Transferase (GST-4) and enzyme gamma-glutamyl cysteine synthetase (GCS-1), which plays a role in catalysis of glutathione respectively [54].

## **2.7 Effect of environmental factors on oxidative stress response**

*C. elegans* present in a stress-free environment with enough food have their redox cycle in balance. The excess ROS species used in signaling pathways are quenched by corresponding antioxidant enzymes [54]. However, animals can be exposed to several forms of stress simultaneously and must adapt to the environment to prioritize survival, development and reproduction [57]. Hence, environmental perturbations can also drive the oxidative stress response mounted by *C. elegans* to xenobiotics. Environmental variables such as changes in external temperature, caloric restriction, and light can also trigger oxidative stress and SKN-1 dependent response pathways [29], [58], [59].

When the worms are under heat stress, HSF-1 transcription factor linked expression of different heat shock proteins has been observed [58]. These heat shock proteins help prevent misfolding of proteins caused due to the thermal stress and restore proteostasis [60]. Parallely, localization of SKN-1: GFP in cell nuclei upon application of heat has also been observed [61]. This suggests a mechanism for crosstalk between heat stress and oxidative stress responses. Interestingly, Crombie et al identified antagonistic interaction between HSF-1 driven heat stress response pathway and SKN-1 driven oxidative stress response pathway [62]. They hypothesize that heat stress application results in decoupling of SKN-1 accumulation and downstream target gene transcription. Similarly, there has been a cross regulation between SKN-1 and DAF-16 transcription factor, the worm FOXO protein ortholog [63]. DAF-16 is the main regulator of the Insulin/ IGF-1 signaling (IIS) pathway known to influence lifespan, early stage, and late stage health [64]. Dietary restriction, (ie) restriction in food intake without malnutrition, is known to

influence both the transcription factors [65]. Tullet et al. observed an up regulation of SKN-1 similar to DAF-16 with a decrease in IIS [66]. An isoform of SKN-1 (SKN-1b) is expressed in the ASI neurons under dietary restriction [59]. Intermittent fasting is known to extend the lifespan of *skn-1* mutants [67]. These studies indicate that dietary restriction also plays a role in driving these responses through the IIS pathway. Studies involving simultaneous exertion of oxidative stress, heat stress, and dietary restriction have not been reported yet.

### **2.8 *gst-4* as a reporter of the SKN-1 pathway**

Tawe et al. used differential RT-PCR display to identify gene expression in response to paraquat, a cytotoxic herbicide known to induce oxidative stress [68]. GSTs were identified to have higher activity under such stress. GST catalyze conjugation of glutathione with xenobiotics. Glutathione (GSH) is an intracellular thiol used by cells to protect against xenobiotics. It is composed of three amino acids, glutamate, cystine, and glycine. There is a peptide linkage between cysteine and glycine and covalent bond between the gamma carboxyl group of the glutamate and amino group of cysteine. In the oxidized state it forms a disulphide (GSSG). ROS, alpha, beta-unsaturated aldehydes, electrophilic compounds interact with GSH, altering cell's reduction capability. Different oxidative stressors such as exposure to quinones, H<sub>2</sub>O<sub>2</sub>, hyperbaric oxygen elicit different spectrum of glutathione response in *C. elegans*. Glutathione response can be tracked *in vivo* using the transgenic strain CL2166 (dvIs19 III) created by Link et al [69]. GFP expression is controlled by a 727 base pair Ce-GST-p24 promoter region. It was observed that there was increased expression of GFP in worms stressed with compounds such as paraquat, while external ROS generated by hypoxanthine/XOD system, UV light, and heat did not elicit a response [70]. It should be noted that there are other methods to track GSH, such as high-performance liquid chromatography (HPLC), using DTNB dye reaction. However, these methods require laborious

protocols and worms to be lysed as mentioned in the above section [71]. The CL2166 strain, which has GFP tagged to the promoter region of *gst-4*, has been used as a reporter for SKN-1 induced oxidative stress response [54], [71], [72]. Dose dependent and time dependent *gst-4* responses to oxidative stressors such as paraquat, acrylamide have been observed [33], [34]. The *gst-4* gene response is dependent on other stressors such as heat stress and dietary restriction [62],[73]. This makes the CL2166 strain a well-suited candidate studying response to simultaneous stresses. Given that CL2166 has also been used in high throughput screening for small molecule inhibitors of the SKN-1 pathway, it is also possible to scale up simultaneous exposure experiments [49].

## **2.9 Design of Experiments (DoE) approach**

A properly designed and randomized experimental run can determine causation whereas an observational study can establish only correlation and not causation [23][74]. Fisher is credited as the person for laying the foundations of modern statistics and for introducing DoE approach in science and industry. The initial DoE approaches were used by Fisher to conduct experiments in the field of agriculture. Traditional experimentation where each factor is studied independent of the other is called One-Factor-At-a-Time (OFAT) experiments. This is considered a disadvantage since we lose the information regarding interactions which might happen at conditions with multiple exposures. DoE enables us to study interactions between the factors. Other advantages include maximizing process knowledge utilizing minimum resources, establishing relationships between actors in an efficient manner.

DoE approach has been used sparsely in *C. elegans* research. Lucio et al utilized DoE to optimize preparation of nanoparticle carriers for glibenclamide to perform *in vivo C. elegans* study [75]. The nanoparticles were delivered orally to the animals and a maximum of 15% reduction in

fat content was recorded. Letizia et al. employed DoE to study the influence of doxycycline on the animals' development at different drug concentration, temperature and feeding routine [76].

## 2.10 Mixture model and optimal design

Mixture experiments require the individual factors to totaling to a constant value. In general cases they add up to one [74]. Thus, the factors' levels cannot vary independently in mixture experiments. The statistical model developed in a mixture design is different from the standard main effects model used in the factorial design. The intercept or constant term found in the main effects model is not included in the mixture design, since that would be linearly dependent on the sum of the mixture components. For a mixture experiment,

$$\sum_{i=1}^q x_i = x_1 + x_2 \dots \dots + x_q = 1 \quad (1)$$

where,  $x_1, x_2, x_3$  represent the proportions of the  $q$  components in the mixture.

The mixture model is thus represented by either the first order or second order Scheffé model (Eq. 2)

$$Y = \sum_{i=1}^q \beta_i x_i + \sum_{i=1}^{q-1} \sum_{j=i+1}^q \beta_{ij} x_i x_j + \varepsilon \quad (2)$$

where,  $Y$  represents the response,  $\beta_i, \beta_{ij}$  represent the parameter estimates,  $\varepsilon$  represents the error in the model.

For mixture experiments where the process variables also change, the Scheffé model is combined with a main effects model which also accounts for the interactions between the process variables. Based on the number of possible runs, other models have been proposed by Prescott, Kowalski et al.

The optimal design for the first order Scheffé model is a simplex lattice model where only the pure components are considered. Since the sum of components is fixed, the design takes a "slice" of the response space as shown in figure 2.3. Generally, mixture designs are represented in

the  $\{q,m\}$  simplex-lattice design for  $q$  components defined by the coordinate setting with proportions assumed by each component to take  $m+1$  equally spaced values from zero to one. The simplex lattice designs are boundary point designs. For example, in a three-component mixture with three equal proportions, there are 10 points that would be considered as shown in figure 2.4a. However, all the design points are located at the boundary and no interior points are considered. A simplex centroid design accounts for the interior points too. In a  $q$ -component simplex-centroid design, the number of distinct points is  $2^q - 1$ . These correspond to “ $q$ ” single component points,  $(qC_2)$  combination of binary mixtures and  $(qC_3)$  combinations of ternary mixtures. For a three-component mixture, we have three individual points, three binary mixtures and one ternary mixture point as shown in figure 2.4b.

However, it is generally impossible to run all the points of the mixture experiments under homogeneous circumstances in a single batch. Block effects and split plots can be included in the mixture model to account for the effects of other factors which cannot be controlled between multiple batches. The optimal design for the Scheffé model along with block effects/split plot has to be generated using statistical software packages such as JMP, R, design expert etc.

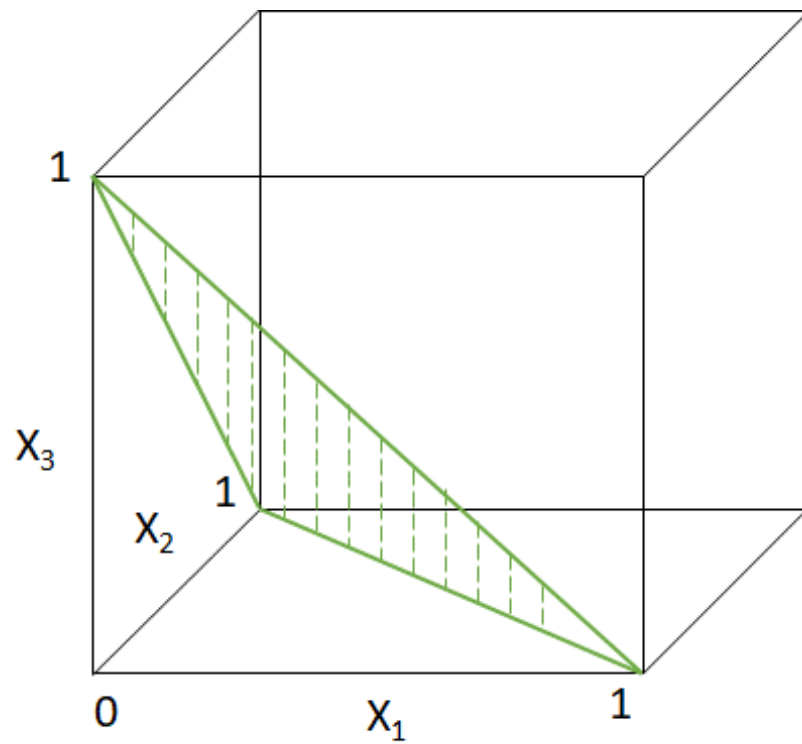


**Figure 2.3. Simplex lattice design for a first order Scheffé model is a “slice” of the response space since the sum of the components is fixed. (Goos, 2009)**

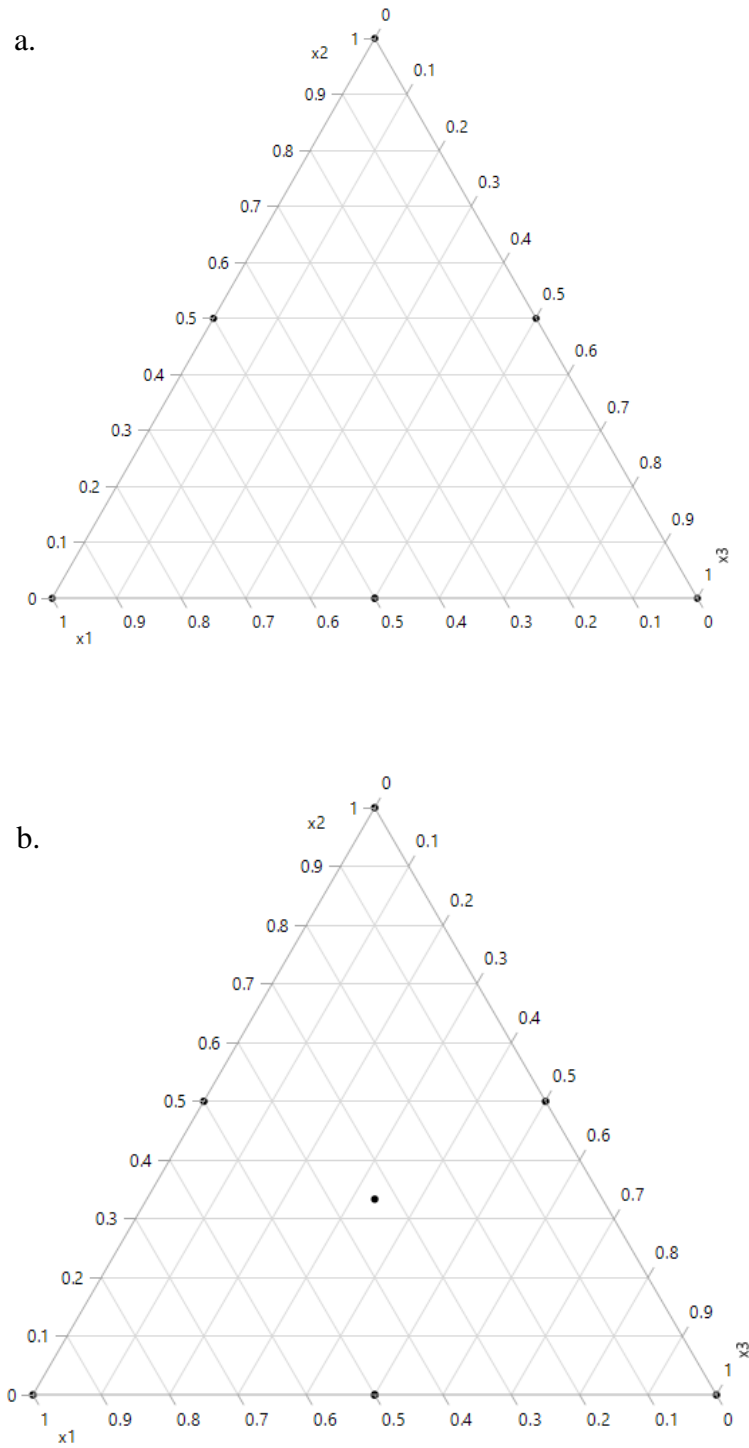


**Figure 2.4. a. Simplex lattice design for a second order Scheffé model b. Simplex centroid design for special Scheffé model**

## 2.11 Optimal design generation in JMP

The optimal mixture designs can be generated using JMP Pro v. 14.2. The custom design function used to produce the optimal design captures and analyzes all important factors and corresponding interactions. The custom design function uses coordinate-exchange algorithm to optimize D-optimality criterion [22], [77]. The D-optimality criterion minimizes the determinant of the covariance matrix of the model coefficient estimates [74]. It is suitable for experiments that focus on estimating effects or testing for significance and for identifying active factors. Two metrics must be specified in the custom design function - number of starts and design search time. The “number of starts” is the number of times that the coordinate-exchange algorithm initiates with a new design and can be specified in the custom design function. A custom design function with a larger “number of starts” has a better possibility of converging onto an optimal design. Design search time determines the number of designs constructed randomly from the starting design. A longer search time improves the optimality of the final generated design. Custom design has diagnostic variables including average variance of prediction to compare different designs. It is based on Fraction of Design space plots [23].

## CHAPTER 3 MATERIALS AND METHODS

In this chapter the methods employed to maintain the strain, prepare the chemicals, select the design, perform the microscopy to capture the images, post process the images, and perform statistical analysis are discussed. The worms and bacterial food used to feed the worms are prepared based on the section 3.1 and the chemical stock are maintained as described in section 3.2. The experimental design generation and selection methodology used for the running the two experiments are described in section 3.3. Once, the design is selected, the age-synchronized worms are exposed to either individual or simultaneous oxidative stress, dietary restriction and heat stress for a period of 8 hours based on the design. The worms are then recovered and imaged using an inverted scope using the method described in section 3.3. The images are then processed, and statistical analysis is performed to infer results from the experiments.

### 3.1 Strain maintenance

*C. elegans* was maintained on standard Nematode Growth Medium (NGM) plates seeded with OP50 *E. coli* bacteria and maintained at 25°C. The strain used in the experiments is CL2166 dvLs19 (*gst-4P::GFP::NLS*). Animals were exposed to either vehicle control or naphthoquinone mixtures in liquid culture (S-medium) in the presence of HB101 bacteria based on established procedures [78]. HB101 *E. coli* bacteria was grown in LB growth media in the presence of 4 mM streptomycin. The bacteria were washed thrice with SB media and pelletized and resuspended in S Media at a concentration of 100 mg/mL.

### 3.2 Chemical Preparation

Juglone, naphthoquinone, and plumbagin were sourced from Fisher Scientific and stored appropriately. 100 mM Stock solutions were prepared for naphthoquinone and plumbagin by

dissolving the powdered compounds in DMSO and is stored at  $-20^{\circ}\text{C}$ . Juglone stock was prepared fresh before the start of each experiment.

### 3.3 Design generation

The first design for the chemical mixtures of juglone, naphthoquinone, and plumbagin included 40 runs in 10 blocks of 4 runs each. Block effect accounts for using different population of worms (i.e., biological samples). A vehicle control was run along with each block to account for the differences in the populations due to minor changes in the growth conditions such as plates used, ambient temperature, etc. Vehicle control response is plotted using an X-bar (average) and S (standard deviation) control chart. A simplex centroid design and a JMP generated design were analyzed to check the effect of oxidant mixtures at *ad libitum* feeding conditions ( $2 \times 10^{10}$  cells/mL) and no heat stress conditions. The JMP design was generated with 100 starts and a generation period of 60 minutes to get the design points (i.e. mixture proportions). The generated design had 21 different design points in the design space and an average variance of prediction of 0.363. The simplex centroid design had an average variance of prediction of 0.367. The increase in variance of prediction between the simplex and the JMP generated design was 0.004. The simplex centroid design was chosen as the mixture proportions can be prepared easily and allows multiple replication at the design points compared to the generated design.

A second mixture design was generated to account for the effects of the heat stress and dietary restriction on the naphthoquinone mixtures. Two levels of heat exposures:  $20^{\circ}\text{C}$  and sublethal  $33^{\circ}\text{C}$  were considered as the first process variable. Two levels of HB101 bacterial diet regime - *Ad libitum* ( $2 \times 10^{10}$  cells/mL) and dietary restriction ( $2 \times 10^9$  cells/mL) was considered as the second process variable [79]. A split plot design was used to account for the four different combinations of heat stress and dietary restriction. A random design was generated for 84 runs

with number of starts as 100 and design search time of 60 mins. The 84 runs were distributed into 28 split plots with 3 runs each. Each split plot had a specified heat stress and diet level. The design had an average value of prediction 0.1799. The design was compared with an equally replicated simplex centroid design with an average value of prediction of 0.1787. Equally replicated simplex centroid design was chosen due to a smaller average value of prediction and triple replications at each design point. For each split plot, a split plot level vehicle control was used to ascertain the effect of the process variables. An overall vehicle control at process conditions 20°C and *ad libitum* diet was used to compare the 28 populations. The overall vehicle controls were plotted as Xbar and S control chart. Experimental control was used to find the main effect of process variables - heat stress and dietary restriction.

### **3.4 Application of oxidative stress and fluorescent imaging**

Approximately 30-40 worms were distributed into (each of) 24 well plates containing the oxidant and HB101 bacteria in S-Medium. The control experiments were conducted with an empty vector of DMSO. The worms were exposed to the oxidants for a period of 8 hours at a temperature of  $20\pm 1^\circ\text{C}$ . For imaging, the worms are immobilized using 4mM tetramisole on 2% agarose pads. A dose response for the individual compounds was first performed. The naphthoquinone mixtures were applied based on the designs generated in the previous section. The worms were imaged using a wide field inverted fluorescence microscope Leica DMi8 system at 5x magnification after the exposure period. A spectra X laser illumination system centered at 470 nm was used to excite the integrated GFP. A Hamamatsu Orca Flash 4.0 16-bit digital CCD camera system was used to capture a grayscale 2048 \* 2048-pixel sized image of the fluorescing animals with pixel intensity ranging from 0 - 65535.

### 3.5 Quantitative image processing

The intensity of the GFP driven by the *gst-4* promoter is quantified to estimate oxidative stress response *in vivo*. Gst-4 expression is observed throughout the animal as shown in the figure 3.1a. The images were processed using a custom-made MATLAB script. A binary mask was generated which identifies a single worm per image as shown in figure 3.1b. The MATLAB `regionprops` function was used to quantify the mean intensity of the animal by overlapping the binary mask over the original image as shown in figure 3.1c.

### 3.6 Statistical analysis

The data was compiled and analyzed using JMP Pro v.14.2. The standard least squares second order Scheffe model accounting for the individual components, mixture interactions, effect of the process variables was used. The block effect in the first design and the split plot in the second design were fixed as a random effect.

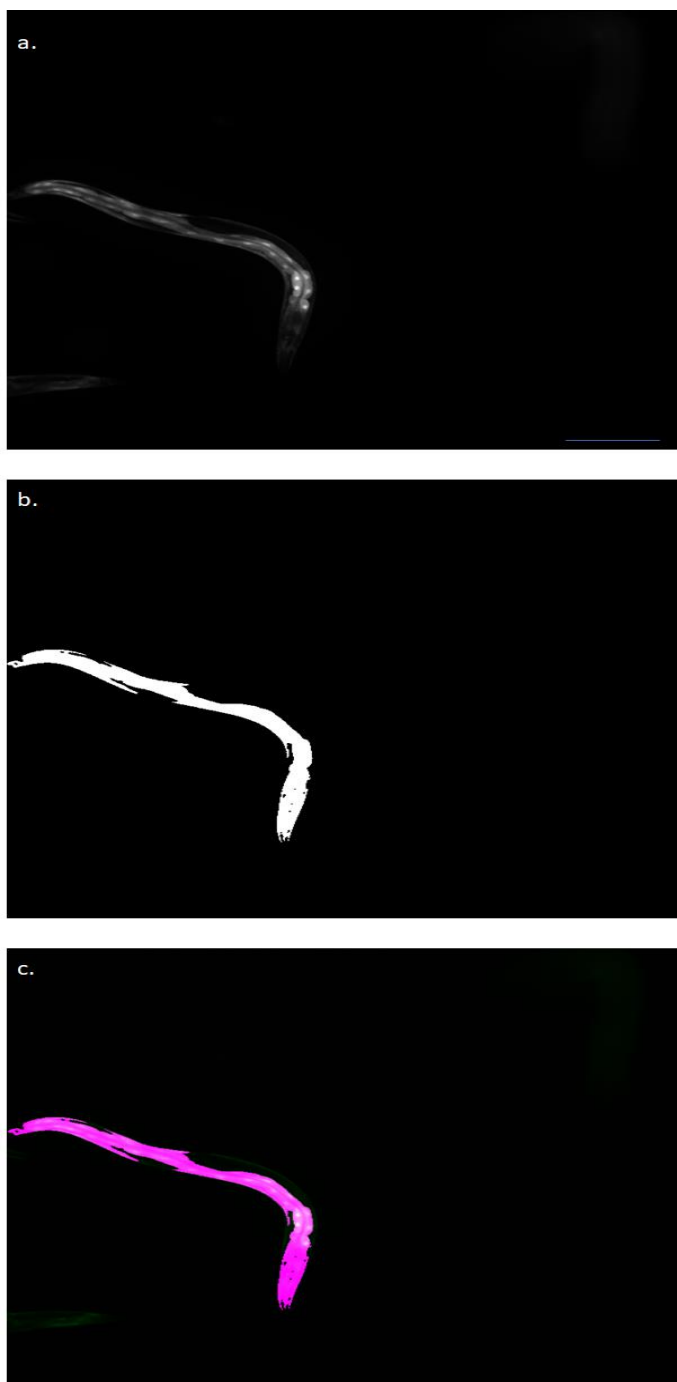


**Figure 3.1. Image Processing methodology. a. Unprocessed image. b. Binary mask c. Overlap of mask onto the image to quantify intensity.**

## CHAPTER 4 RESULTS AND DISCUSSION

### 4.1 Dose dependency

Worms were exposed to the individual compounds for a period of 8 hours. Previous exposure studies with other compounds suggest that a period of 8 hours is sufficient to elucidate a dose dependent *gst-4* response [34]. The worms exhibited a dose dependent response to all 3 compounds as shown in figure 4.1. High doses are considered lethal and are known to reduce lifespan [80]. Sublethal doses in the range of 20-30  $\mu\text{M}$  for the 3 compounds under study is known to drive a SKN-1 pathway dependent *gst-4* response and also induce a hormetic effect driven by the SKN-1 dependent stress response pathway [81], [56]. Future experiments were performed using a sublethal dose of 30  $\mu\text{M}$  to observe differences in response to the mixtures.

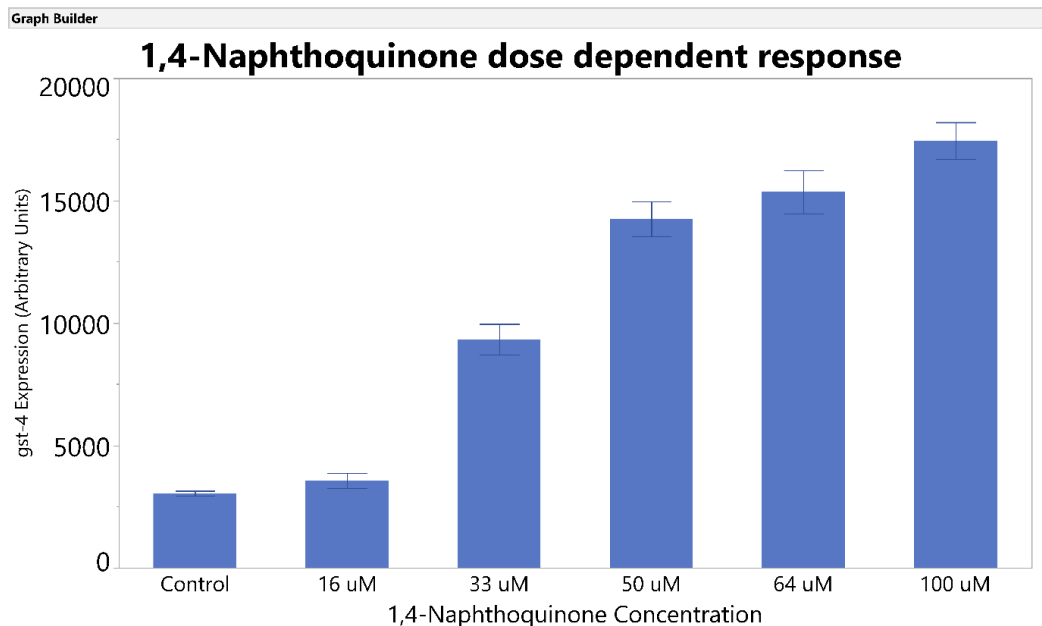


**Figure 4.1. a Dose dependent *gst-4* response to 1,4-Naphthoquinone. (n>30 worms for each concentration level)**

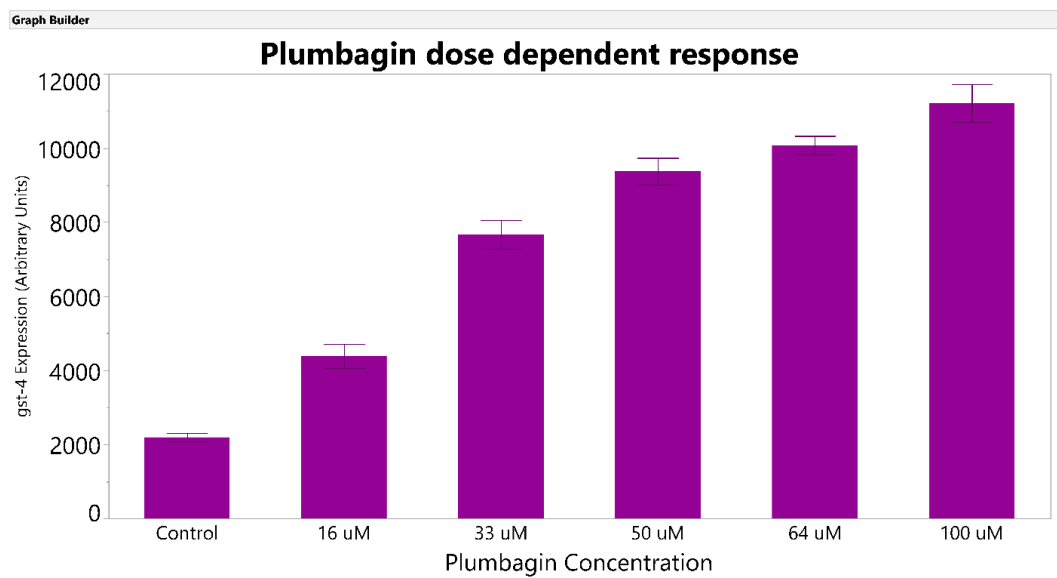


**Figure 4.1. b Dose dependent *gst-4* response to Plumbagin. (n>30 worms for each concentration level)**

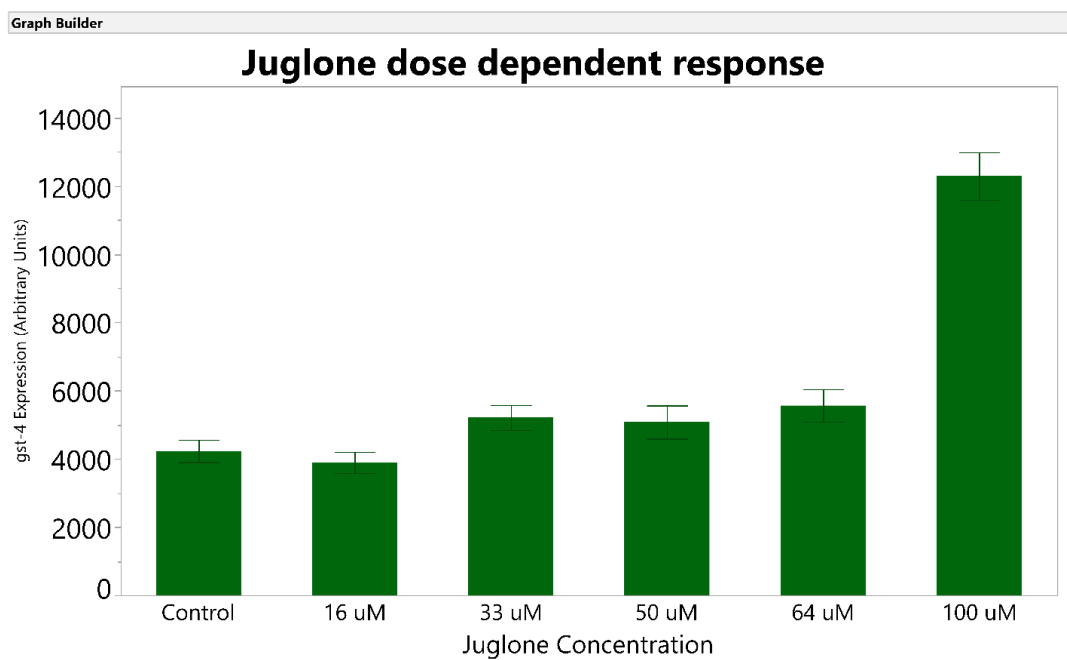


**Figure 4.1. c. Dose dependent *gst-4* response to Juglone. (n>25 worms for each concentration level)**

## 4.2 1,4-Naphthoquinone mixtures under fixed process conditions

The first mixture experiments were performed under *ad libitum* and no heat stress conditions based on the selected design. The vehicle controls simultaneously run with each experiment are shown in figure 4.2 and the response surface to the individual compounds, and the mixture is shown in figure 4.3. The population block effect which accounts for the variation introduced by treatment application process is tabulated in Table 4.1. The tests for significant effects and parameter estimates are tabulated in Table 4.2. A differential response to the mixtures and the individual compounds is observed.

The *gst-4* baseline response of vehicle controls run for each set of experiments indicates that the worms of subsequent populations are in statistical control and are comparable to each other. However, the block effect included in the mixture model to also account for the same indicates that the experiments 4, 6, 10 had a significant effect. This can be attributed to other lurking factors in the experimental treatment application process. Adding the block effect has prevented potential confounding caused by the lurking factors on the mixture effects. Figure 4.3 shows that the individual naphthoquinones have a higher *gst-4* response compared to mixtures. Both binary and ternary mixtures don't have a similar effect on the *gst-4* response. There are differences in the reactivity of the juglone and plumbagin based on electrochemical studies [46]. Inbaraj et al. reported differences in the mechanism of the toxicity by juglone and plumbagin in HaCaT Keratinocytes [10]. Hunt et al. also observed differences in *C. elegans* oxidative stress response depending on the nature of the naphthoquinone compounds [81]. Bhatla et al. observed a difference in detection of oxidative stressors by the I2 neuron implicated in the detection of oxidative stress. Sublethal levels of H<sub>2</sub>O<sub>2</sub> activated the I2 neuron while paraquat did not elucidate any response until a very high dose was delivered [82]. The other neurons implicated in the detection of

oxidative stress are yet to be deduced. The difference in the *gst-4* response to the individual compounds and the mixtures can be potentially attributed to the combined effect of detection and the mechanism of toxicity by the different naphthoquinones.

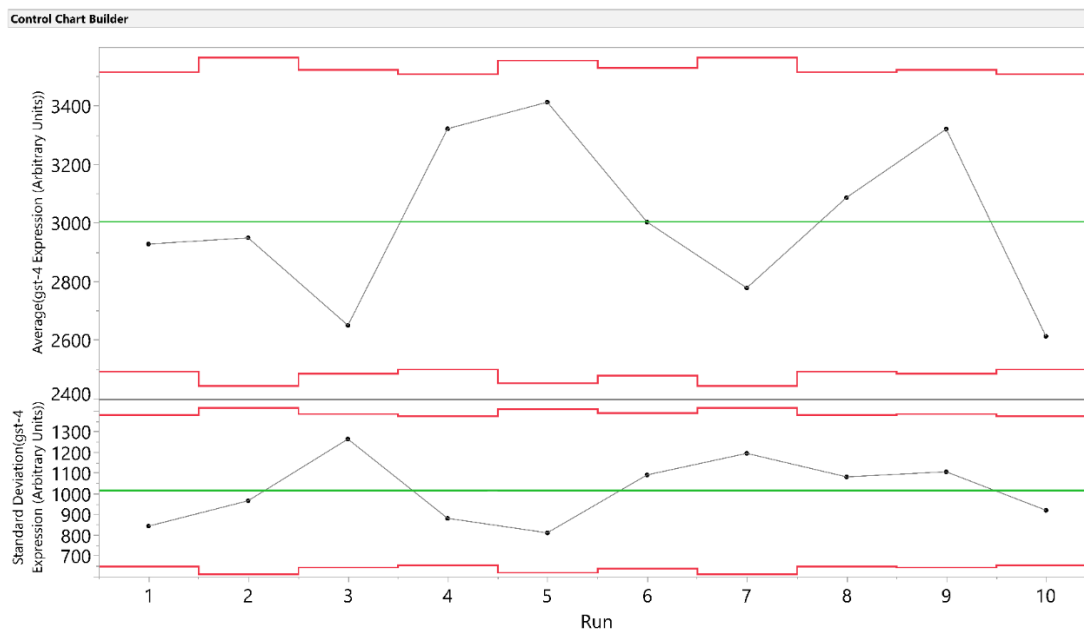


**Figure 4.2. Control chart of the 10 populations used to perform the first mixture experiment.**

**Table 4.1. Effect of experimental treatment application process on the first experiment**

Response <i>gst-4</i> Arbitrary Expression					
Random Effect Predictions					
Term	BLUP	Std Error	DFDen	t Ratio	Prob> t
Population Block[1]	275.36561	321.8492	20.79	0.86	0.4020
Population Block[2]	300.83352	322.62	20.75	0.93	0.3618
Population Block[3]	-73.13189	321.918	20.79	-0.23	0.8225
Population Block[4]	724.30893	322.62	20.75	2.25	0.0358*
Population Block[5]	332.85638	322.62	20.75	1.03	0.3141
Population Block[6]	-1076.835	322.5951	20.81	-3.34	0.0031*
Population Block[7]	161.88264	321.1286	20.77	0.50	0.6195
Population Block[8]	165.11411	321.8492	20.79	0.51	0.6133
Population Block[9]	-119.8882	321.4297	20.75	-0.37	0.7129
Population Block[10]	-690.5058	322.9633	20.79	-2.14	0.0446*

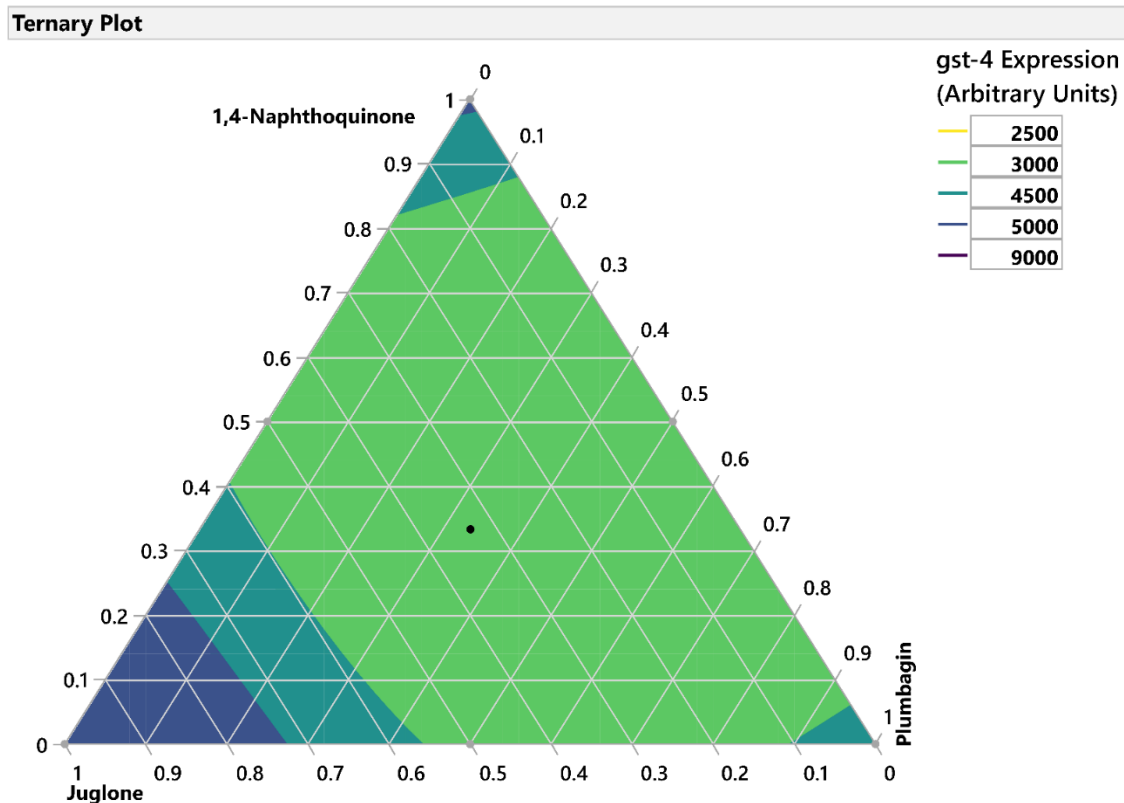


**Figure 4.3. Response surface of first mixture response.**

**Table 4.2. Testing for significant effects in first mixture experiment.**

Response gst-4 Arbitrary Expression					
Parameter Estimates					
Term	Estimate	Std Error	DFDen	t Ratio	Prob> t
Juglone(Mixture)	6647.0502	339.8023	29.88	19.56	<.0001*
Naphthoquinone(Mixture)	5221.8169	339.8023	29.88	15.37	<.0001*
Plumbagin(Mixture)	4767.0292	316.8838	27.64	15.04	<.0001*
Juglone*Naphthoquinone	-7270.802	1308.749	25.49	-5.56	<.0001*
Juglone*Plumbagin	-4855.491	1262.854	25.02	-3.84	0.0007*
Naphthoquinone*Plumbagin	-6065.188	1269.632	25.14	-4.78	<.0001*
Juglone*Naphthoquinone*Plumbagin	10021.036	8789.285	25.07	1.14	0.2650

### 4.3 1,4-Naphthoquinone mixtures under changing process conditions

Temperature and dietary intake have been hypothesized to affect the oxidative stress response in *C. elegans* [56], [83]. To study the effect of temperature and dietary restriction on the oxidative stress response to 1,4-Naphthoquinone mixtures, we used simplex centroid design with

the 84 runs separated as 21 split plots. An experimental and overall control was run parallelly with each split plot to study the main effect of process parameters separately. Figure 4.4 plots the experimental control that was run to study the main effect of dietary restriction and heat stress. Figure 4.5 plots the control chart of the overall controls run at *ad libitum* and no heat stress. The overall controls were run to compare the 21 populations used for each of the split plot.

As seen in figure 4.4, heat stress and dietary restriction significantly affect the *gst-4* oxidative stress response, with the response having a lower value than overall controls. The reduction in *gst-4* expression levels by heat stress is attributed to prioritization to upregulate heat stress proteins over oxidative stress proteins [62]. The reduction in *gst-4* level by dietary restriction can be attributed to reduced activity of *cct-4* under dietary restriction [73]. *cct-4* encodes for a chaperonin directly involved in SKN-1–dependent transcription of *gst-4* [73]. The points will be replicated soon to reduce the influence of population used on response. Table 4.3 shows that there are no differences between population blocks indicating that there is no significant variation caused by the experimental treatment application process. The *gst-4* response to 1,4-Naphthoquinone mixtures under different process conditions is shown in figure 4.6. The main effects & interaction tested for significance is presented in table 4.4. The *ad libitum* and 20°C (top left) response surface in figure 4.6 is the recreation of the mixture experiment 1 and it has the same profile as before. As we increase the temperature to 33°C, heat stress flattens the *gst-4* response to the individual components and binary, ternary mixtures. The heat stress response is predominant. This is in line with the previously observed results [62]. In contrast, as we reduce the food concentration, we observe that dietary restriction exhibits a significant synergistic effect with the oxidative stress response to juglone, binary and ternary mixtures, but not with individual naphthoquinone and plumbagin. At lower concentration and higher temperature of 33°C, the heat stress response still

predominates and the synergistic interaction with the dietary restriction seen at 20°C is not replicated.

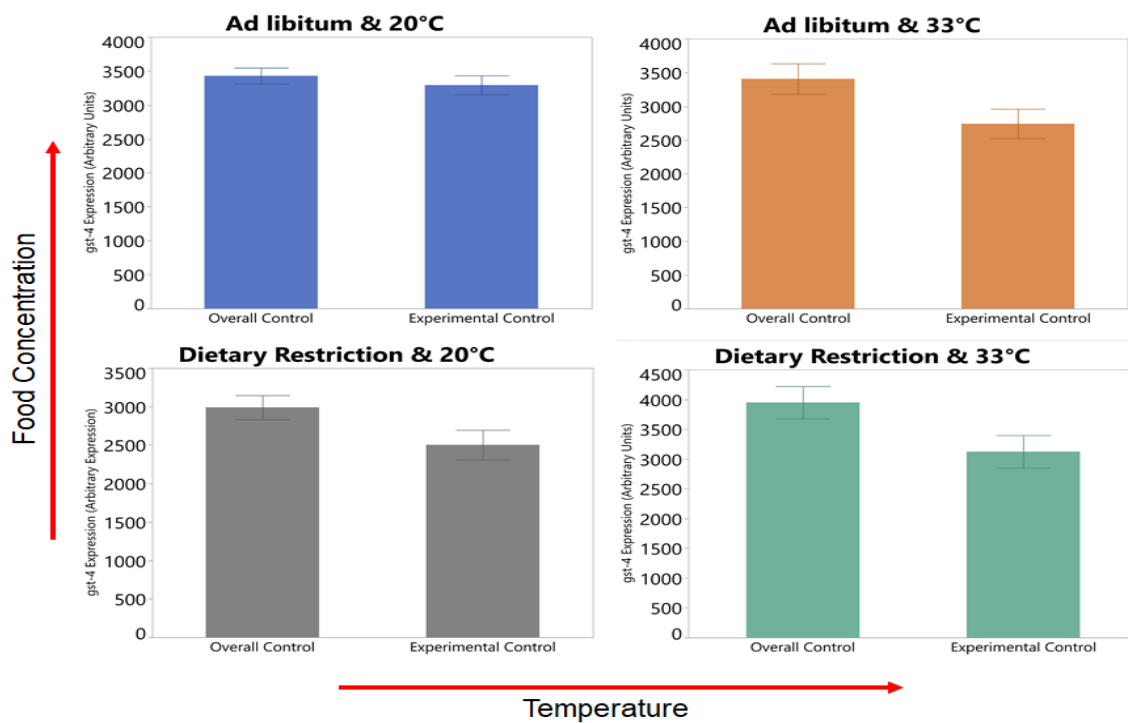


**Figure 4.4. Testing for main effects of process variables.**

**Table 4.3. Effect of experimental treatment application process on the second experiment.**

Response Response					
Random Effect Predictions					
Term	BLUP	Std Error	DFDen	t Ratio	Prob> t
Whole Plots[1]	54.050391	393.6369	8.544	0.14	0.8940
Whole Plots[2]	-85.82942	393.8921	8.481	-0.22	0.8327
Whole Plots[3]	-282.9799	393.6385	8.544	-0.72	0.4914
Whole Plots[4]	-8.467667	389.2808	9.044	-0.02	0.9831
Whole Plots[5]	848.851	390.5736	9.058	2.17	0.0576
Whole Plots[6]	61.574766	393.691	8.525	0.16	0.8794
Whole Plots[7]	201.24976	391.1333	8.865	0.51	0.6195
Whole Plots[8]	109.89684	391.0957	8.88	0.28	0.7851
Whole Plots[9]	-82.89563	389.7043	8.969	-0.21	0.8363
Whole Plots[10]	0.331235	391.9548	8.831	0.00	0.9993
Whole Plots[11]	-335.0906	393.6212	8.534	-0.85	0.4178
Whole Plots[12]	-134.9743	391.9898	8.825	-0.34	0.7387
Whole Plots[13]	-140.562	391.0951	8.88	-0.36	0.7277
Whole Plots[14]	-134.1268	393.85	8.487	-0.34	0.7417
Whole Plots[15]	-106.2243	395.4876	8.237	-0.27	0.7948
Whole Plots[16]	36.024148	392.515	8.641	0.09	0.9290
Whole Plots[17]	110.26851	413.961	7.183	0.27	0.7974
Whole Plots[18]	80.883863	390.5736	9.058	0.21	0.8405
Whole Plots[19]	-124.6995	390.5736	9.058	-0.32	0.7568
Whole Plots[20]	509.51374	391.4018	8.859	1.30	0.2258
Whole Plots[21]	-535.4545	393.0081	8.583	-1.36	0.2077
Whole Plots[22]	-638.3822	391.9594	8.83	-1.63	0.1385
Whole Plots[23]	-8.208652	392.1464	8.794	-0.02	0.9838
Whole Plots[24]	-36.7241	392.7312	8.624	-0.09	0.9276
Whole Plots[25]	369.34377	389.0444	9.04	0.95	0.3671
Whole Plots[26]	-132.5801	392.0765	8.818	-0.34	0.7432
Whole Plots[27]	-174.5368	391.1823	8.896	-0.45	0.6661
Whole Plots[28]	579.74846	395.4876	8.237	1.47	0.1798

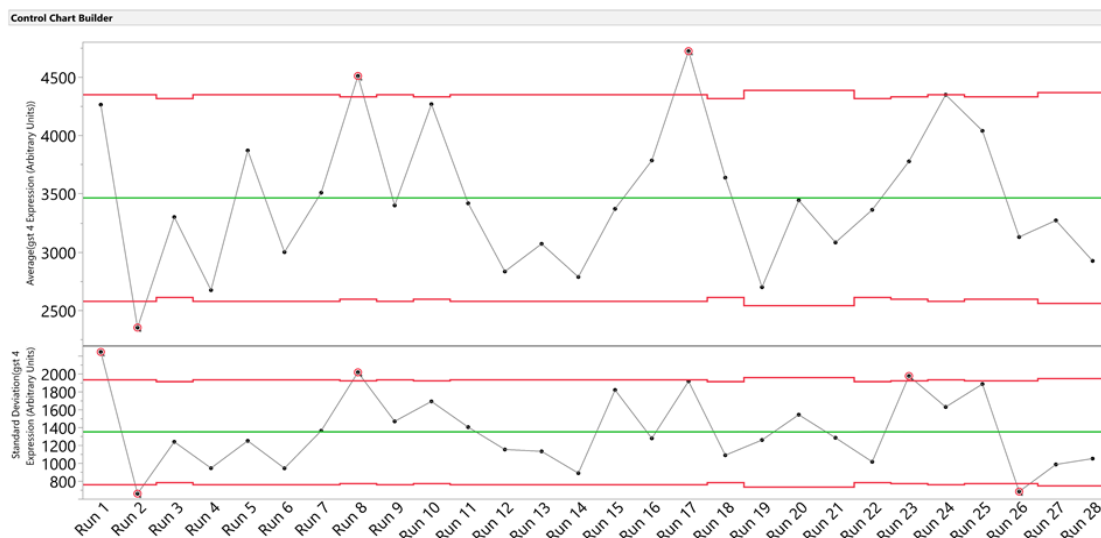


**Figure 4.5. Control chart of the 28 populations used to perform the second mixture experiment.**

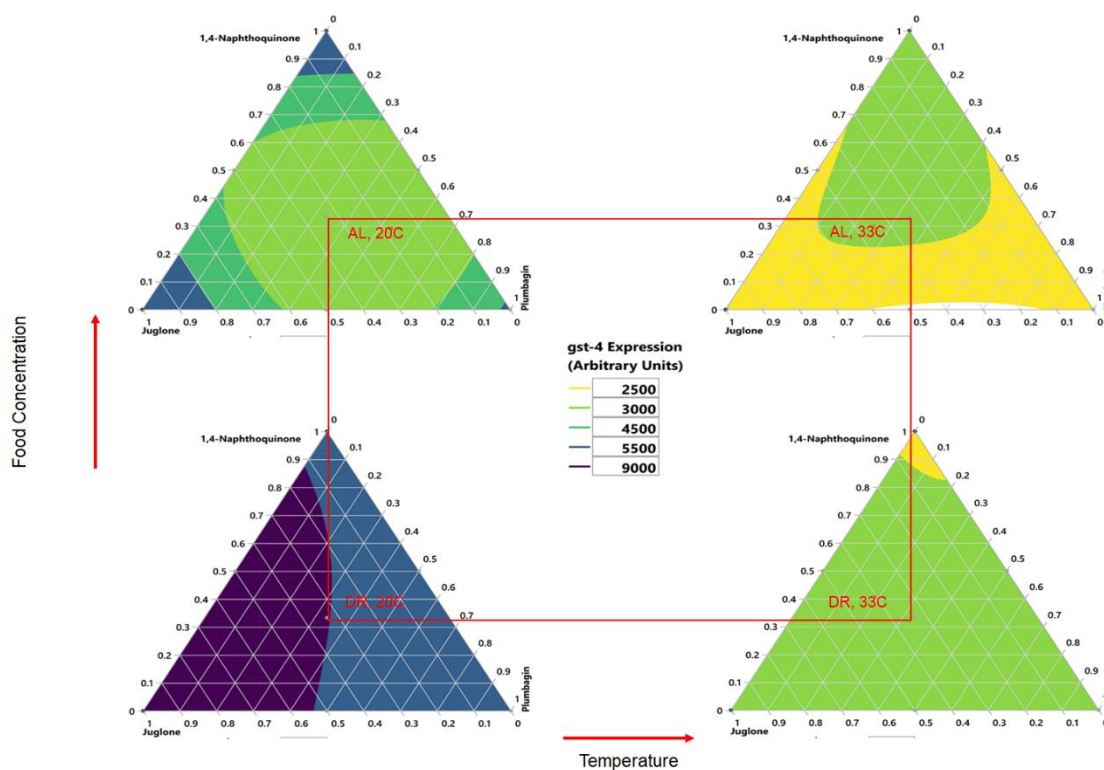


**Figure 4.6. Effect of process variables on the oxidative stress response to 1,4-Naphthoquinone mixtures.**

(AL - *Ad libitum*, DR - Dietary restriction)

**Table 4.4. Testing for significant effects in second mixture experiment.**

Term	Estimate	Std Error	DFDen	t Ratio	Prob> t
Juglone(Mixture)	6177.8389	275.5169	55.86	22.42	<.0001*
Naphthoquinone(Mixture)	5298.7125	275.8681	55.93	19.21	<.0001*
Plumbagin(Mixture)	4472.3013	275.5572	55.87	16.23	<.0001*
Juglone*Naphthoquinone	-1381.237	1299.569	47.69	-1.06	0.2932
Juglone*Plumbagin	-2578.32	1274.236	43.16	-2.02	0.0493*
Juglone*Dietary level	-1034.071	275.5169	55.86	-3.75	0.0004*
Juglone*Heat Stress level	-2820.273	275.5169	55.86	-10.24	<.0001*
Naphthoquinone*Plumbagin	-1551.95	1279.763	43.69	-1.21	0.2318
Naphthoquinone*Dietary level	-202.2865	275.8681	55.93	-0.73	0.4665
Naphthoquinone*Heat Stress level	-2206.305	275.8681	55.93	-8.00	<.0001*
Plumbagin*Dietary level	-307.1387	275.5572	55.87	-1.11	0.2698
Plumbagin*Heat Stress level	-1620.904	275.5572	55.87	-5.88	<.0001*
Dietary level*Heat Stress level	-627957.8	3321914	43.25	-0.19	0.8509
Juglone*Naphthoquinone*Plumbagin	-170.4261	8971.847	43.25	-0.02	0.9849
Juglone*Naphthoquinone*Dietary level	-4367.79	1299.569	47.69	-3.36	0.0015*
Juglone*Naphthoquinone*Heat Stress level	1411.8196	1299.569	47.69	1.09	0.2828
Juglone*Plumbagin*Dietary level	-2798.803	1274.236	43.16	-2.20	0.0335*
Juglone*Plumbagin*Heat Stress level	1544.7989	1274.236	43.16	1.21	0.2320
Juglone*Dietary level*Heat Stress level	628648.33	3321895	43.25	0.19	0.8508
Naphthoquinone*Plumbagin*Dietary level	-3076.211	1279.763	43.69	-2.40	0.0205*
Naphthoquinone*Plumbagin*Heat Stress level	1855.7684	1279.763	43.69	1.45	0.1542
Naphthoquinone*Dietary level*Heat Stress level	628406.73	3321898	43.25	0.19	0.8508
Plumbagin*Dietary level*Heat Stress level	628042.92	3321893	43.25	0.19	0.8509
Juglone*Naphthoquinone*Plumbagin*Dietary level	6861.8438	8971.847	43.25	0.76	0.4485
Juglone*Naphthoquinone*Plumbagin*Heat Stress level	-232.7713	8971.847	43.25	-0.03	0.9794
Juglone*Naphthoquinone*Dietary level*Heat Stress level	3316.2543	1299.569	47.69	2.55	0.0140*
Juglone*Plumbagin*Dietary level*Heat Stress level	2294.6879	1274.236	43.16	1.80	0.0787
Naphthoquinone*Plumbagin*Dietary level*Heat Stress level	2582.8949	1279.763	43.69	2.02	0.0497*

#### 4.4 Discussion

Naphthoquinones are industrially relevant compounds known to elicit toxicity through oxidative stress [39], [8], [45], [46]. The naphthoquinones of the same family have different activity in the in vitro and in vivo models [9]. This can be accredited to the distinct mechanisms adopted by the different naphthoquinones to elicit oxidative stress [10], [44], [81]. Such differences in mechanism of toxicity can combine either synergistically or antagonistically in mixture forms as seen in other chemical and biological systems [5], [6]. This interaction effect can be potentially confounded by the total volume of the mixture if the experiments are not designed properly [23]. Using mixture designs has enabled us to gain knowledge of the *C.elegans gst-4* response to 1,4-naphthoquinone mixtures over different process conditions without confounding by the total volume of oxidant mixture.

Figure 4.1 plots the dose dependent response mounted by the animals to individual components. We see that as the naphthoquinone concentration increases the *gst-4* activity also increases and saturates as observed in previous studies [33], [34]. Glutathione-S-Transferase (GST) enzyme catalyzes Michael's addition of glutathione with xenobiotic stressor [54]. The saturation could indicate maximum transcription of the gene at the young adult stage and further oxidative stress would not elicit a higher response. We hypothesized that a synergistic response would be observed to mixtures and saturation of the response would prevent us to compare the activity to the different proportions of the mixtures. Hence, we conducted the mixture experiments at lower dose of 30 uM. Unexpectedly, we observed an antagonistic response to the binary and ternary mixtures as shown in the figure 4.3. This can be attributed to the different mechanisms of toxicity elicited by the components of the mixture. From figure 4.3, we observe that the 30 uM of juglone has the highest *gst-4* response of the individual components. Juglone has relatively higher

chemical activity and could undergo Michael's addition to glutathione even at the lower doses [45], [46]. 30  $\mu$ M of 1,4-Naphthoquinone and plumbagin could cause oxidative stress through redox cycling at the lower doses, and only at higher doses cause Michael's addition to glutathione [44], [46]. Hence, the binary and ternary mixtures might have a lower activity. This indicates that the individual components do not act synergistically through a singular mechanism and baseline activity of *gst-4* and other detoxification genes is sufficient to combat the oxidative stress caused by the mixtures.

Environmental conditions can alter both the mixtures toxicity mechanism as well as the response mounted by the animals to combat the xenobiotic stressors [7]. Understanding such a response is pertinent as oxidative stress induced by xenobiotic compounds could potentially play a significant role in progression of neurodegenerative diseases [12], [30], [31]. *C.elegans* present in a hostile environment have to prioritize survival over growth and reproduction [62]–[64]. This translates as upregulation of genes involved in stress response pathways such as those regulated by HSF-1 and SKN-1 [54], [58].

Figure 4.6 presents the four different response surfaces to simultaneous exposure to mixtures, heat stress and dietary restrictions. The top left response surface of figure 4.6 corresponds to only oxidative stress. As seen in Figure 4.3, the individual compounds have a higher response than mixtures. As we reduce the availability of food, the worms undergo dietary restriction. This results in translocation of DAF 16 to the nucleus, which further regulates various genes involved in the SKN-1 oxidative stress response pathway indicating cross talk between the pathways [63], [64]. Simultaneous dietary restriction and oxidative stress has a synergistic effect on the *gst-4* response compared to response mounted by animals which are under dietary restriction alone as shown in figures 4.6 and figure 4.4 (bottom left) respectively. Different genes are down

regulated by reduction in the availability of food. The downregulation of *cct-4* chaperonin in particular, that encodes for regulation of *gst-4* could be possible explanation for reduced activity of *gst-4* response under only dietary restriction (figure 4.4 ,bottom left) [73]. However, simultaneous dietary and oxidative stress could force the animals to upregulate *gst-4* along with other detoxification response genes resulting in higher response (figure 4.6, bottom left) [63], [64]. However, we do not see the synergistic response mounted to pure plumbagin and 1,4-naphthoquinone under dietary restriction. Further experimentation tracking other detoxification genes is necessary to understand such differences in toxicity mechanism of naphthoquinone mixtures.

The *gst-4* response mounted by *C.elegans* to heat stress and simultaneous heat stress and dietary restriction is shown in figure 4.4 (Top Right) and figure 4.4 (Bottom Right) respectively. A significant reduction in *gst-4* levels is observed. This has been attributed to prioritization of proteome activity over detoxification [62]. The HSF-1 related heat stress response genes are upregulated to prevent protein misfolding [62]. No response is observed even when the worms are additionally exposed to individual and mixture oxidative stressors as shown in figure 4.6 (Top right) and 4.6 (Bottom right). Such conserved activity further cements the importance placed to heat stress response over oxidative stress response [62].

*C.elegans* are complex in nature and lot of lurking factors such as variation in developmental period, food availability on plate, temperature can potentially affect the response mounted by the animals. It is necessary to control and account for such effect to as the mixture experiments cannot be performed using single population and must be distributed across different populations. Control charts have proven to be useful in plotting the response of vehicle controls and identifying potential erroneous populations which might show a different response. Such

populations can have different biological activity and can affect the results of the experiments being performed. The mixture design points performed with such populations can be repeated to ensure that response recorded is due to the mixture effects. Adding block factors & split plot as random effect to the model also help us isolate potential populations which can have minor differences in the treatment application process.

Thus, using a combination of mixture experiments and control charts we have showcased the differential *gst-4* response mounted to *C. elegans* to oxidative stressor mixtures under different environmental conditions. These results further warrant the need to investigate the different pathways which are affected due to such mixtures. Such studies can help elucidate how the organism selects compounds to detoxify under different environmental circumstances.

## CHAPTER 5 CONCLUSION AND FUTURE DIRECTIONS

### 5.1 Conclusion

In this work, *gst-4* responses of *C. elegans* young adults to 1,4-Naphthoquinone mixtures under different environmental conditions was studied by using mixture designs. There is a differential response to the individual compounds and the mixtures at different conditions. At *ad libitum*, 20°C the individual components have a higher *gst-4* response compared to the mixtures indicating that there are nonlinear additive effects of the mixtures. Altering the environmental conditions by changing the diet level or heat stress invokes different responses. Dietary restriction has synergistic effect with juglone and mixtures on the *gst-4* response. Heat stress exerted by exposing the worms to 33°C suppresses the *gst-4* responses to both individual components and mixtures. These results reveal interplay between oxidative stress response to xenobiotic mixtures and environmental conditions. Future studies as mentioned in the next section can be conducted at different time points to understand temporal oxidative stress response and with other biomarkers to track parallel pathways simultaneously.

### 5.2 Future Directions

The dynamic equilibrium between ROS, antioxidant enzymes and other cofactors in response to spatial and temporal changes in the environment are important in maintaining health and disease-free life. The response mounted by organisms to changes in the environment are multifold in nature. Heat shock factors (HSF) are important in these responses mounted to acute stress. Stressed cells and organisms show an increased synthesis of heat shock proteins (HSP) upregulated by heat shock factors. HSPs act as molecular chaperones preventing protein misfolding and aggregation [84]. HSP-16.2 is one such protein used as a reporter of HSF-1 activity in *C. elegans*, which accumulates in response to heat stress. Similarly, the insulin/IGF-1-like

signaling (IIS) pathway regulates the food storage and growth in *C. elegans*. Several genes such as DAF-2, AGE-1, AKT-1, AKT-2 are ortholog to mammalian genes involved in aging. They are regulated by the IIS pathway. These genes are downregulated in animals under harsh stressful conditions [64]. The activity of the IIS pathway can be tracked using a reporter for DAF-16, the main transcription factor that regulates IIS. DAF-16 is phosphorylated in the absence of the IIS pathway activation, which prevents its translocation to the nucleus and expression of pro-longevity genes [64]. Tracking HSP-16.2 and DAF-16 parallelly to GST-4 can help us understand the influence of oxidative stressor mixtures on HSF-1 and IIS pathways. Tracking all three reporters simultaneously can help us draw conclusions on interplay of the pathways involved in stress response under changing environmental conditions.

The capture of complex relationships between genetic factors when using the DoE approach can prove to be very useful for understanding the response space [85]. Employing recent advancement in other fields such as automated image processing, robotics, along with the DoE approach allow us to optimize biological assays to minimize signal variance and improve the signal to noise ratio. For example, Taylor et al. used partial factorial designs to optimize three radioligand binding assays and three enzymatic assays run on automated robotic platforms [85],[86]. The design optimized assays had considerably higher signal to background ratio, lower variability, lower assay value ratio (AVR) when compared to the original assays. Wrobel et al. employed a screening design to develop an optimized spotting buffer to run microarray analysis on four different cell lines such as HL60, TPA differentiated HL60, 3T3, and F9 [87]. The optimized spotting buffer had yielded stronger signals compared to four commercially available buffers and two commonly used noncommercial buffers on selected substrate surfaces. With the increased use of tools such as microfluidics, image processing, deep phenotyping using machine learning

algorithms, running *C. elegans* assays has become more economical and less laborious[88]–[91]. Benedetto et al. observed age dependent difference in peak resistance to heat stress, oxidative stress, and resistance to infection. They also observed differences in response to milder stressor patterns [63]. Using such advancements can help us track the stress response pathway over the lifespan of the worms to understand the temporal response to 1,4-Naphthoquinone mixtures at both individual worm resolution and at population level.

## REFERENCES

- [1] D. O. Carpenter, K. F. Arcaro, B. Bush, W. D. Niemi, S. Pang, and D. D. Vakharia, “Human health and chemical mixtures: An overview,” in *Environmental Health Perspectives*, 1998, vol. 106, no. SUPPL. 6, pp. 1263–1270.
- [2] T. Backhaus and M. Faust, “Predictive environmental risk assessment of chemical mixtures: A conceptual framework,” *Environ. Sci. Technol.*, vol. 46, no. 5, pp. 2564–2573, Mar. 2012.
- [3] J. M. Braun, C. Gennings, R. Hauser, and T. F. Webster, “What can epidemiological studies tell us about the impact of chemical mixtures on human health?,” *Environ. Health Perspect.*, vol. 124, no. 1, pp. A6–A9, Jan. 2016.
- [4] R. N. Carvalho *et al.*, “Mixtures of chemical pollutants at European legislation safety concentrations: How safe are they?,” *Toxicol. Sci.*, vol. 141, no. 1, pp. 218–233, Sep. 2014.
- [5] V. C. Moser, R. C. MacPhail, and C. Gennings, “Neurobehavioral evaluations of mixtures of trichloroethylene, heptachlor, and di(2-ethylhexyl)phthalate in a full-factorial design,” *Toxicology*, vol. 188, no. 2–3, pp. 125–137, Jun. 2003.
- [6] L. Feng, S. S. Liu, K. Li, H. X. Tang, and H. L. Liu, “The time-dependent synergism of the six-component mixtures of substituted phenols, pesticides and ionic liquids to *Caenorhabditis elegans*,” *J. Hazard. Mater.*, vol. 327, pp. 11–17, Apr. 2017.
- [7] R. Vermeulen, E. L. Schymanski, A. L. Barabási, and G. W. Miller, “The exposome and health: Where chemistry meets biology,” *Science (80-. )*, vol. 367, no. 6476, pp. 392–396, Jan. 2020.
- [8] J. Grolig and R. Wagner, “Naphthoquinones,” in *Ullmann’s Encyclopedia of Industrial*

- Chemistry*, Weinheim, Germany: Wiley-VCH Verlag GmbH & Co. KGaA, 2000.
- [9] P. Fowler, K. Meurer, N. Honarvar, and D. Kirkland, “A review of the genotoxic potential of 1,4-naphthoquinone,” *Mutation Research - Genetic Toxicology and Environmental Mutagenesis*, vol. 834. Elsevier B.V., pp. 6–17, 01-Oct-2018.
- [10] J. J. Inbaraj and C. F. Chignell, “Cytotoxic Action of Juglone and Plumbagin: A Mechanistic Study Using HaCaT Keratinocytes,” *Chem. Res. Toxicol.*, vol. 17, no. 1, pp. 55–62, Jan. 2004.
- [11] P. M. Chege and G. McColl, “Caenorhabditis elegans: A model to investigate oxidative stress and metal dyshomeostasis in Parkinson’s disease,” *Frontiers in Aging Neuroscience*, vol. 6, no. MAY. Frontiers Media SA, 2014.
- [12] W. J. Huang, X. Zhang, and W. W. Chen, “Role of oxidative stress in Alzheimer’s disease (review),” *Biomedical Reports*, vol. 4, no. 5. Spandidos Publications, pp. 519–522, 01-May-2016.
- [13] V. Dias, E. Junn, and M. M. Mouradian, “The role of oxidative stress in parkinson’s disease,” *Journal of Parkinson’s Disease*, vol. 3, no. 4. I O S Press, pp. 461–491, 2013.
- [14] A. K. Corsi, B. Wightman, and M. Chalfie, “A transparent window into biology: A primer on Caenorhabditis elegans,” *Genetics*, vol. 200, no. 2, pp. 387–407, 2015.
- [15] F. Calahorro and M. Ruiz-Rubio, “Caenorhabditis elegans as an experimental tool for the study of complex neurological diseases: Parkinson’s disease, Alzheimer’s disease and autism spectrum disorder,” *Invertebrate Neuroscience*, vol. 11, no. 2. Springer, pp. 73–83, 08-Dec-2011.
- [16] P. Wittkowski *et al.*, “Caenorhabditis elegans As a Promising Alternative Model for Environmental Chemical Mixture Effect Assessment - A Comparative Study,” *Environ.*

- Sci. Technol.*, vol. 53, no. 21, pp. 12725–12733, Nov. 2019.
- [17] A. K. Vingskes and N. Spann, “The toxicity of a mixture of two antiseptics, triclosan and triclocarban, on reproduction and growth of the nematode *Caenorhabditis elegans*,” *Ecotoxicology*, vol. 27, no. 4, pp. 420–429, May 2018.
- [18] C. Lu, K. R. Svoboda, K. A. Lenz, C. Pattison, and H. Ma, “Toxicity interactions between manganese (Mn) and lead (Pb) or cadmium (Cd) in a model organism the nematode *C. elegans*,” *Environ. Sci. Pollut. Res.*, vol. 25, no. 16, pp. 15378–15389, Jun. 2018.
- [19] Z. Y. Yu, D. Q. Yin, and H. P. Deng, “The combinational effects between sulfonamides and metals on nematode *Caenorhabditis elegans*,” *Ecotoxicol. Environ. Saf.*, vol. 111, pp. 66–71, Jan. 2015.
- [20] J. Chen *et al.*, “Comparison of two mathematical prediction models in assessing the toxicity of heavy metal mixtures to the feeding of the nematode *Caenorhabditis elegans*,” *Ecotoxicol. Environ. Saf.*, vol. 94, pp. 73–79, Aug. 2013.
- [21] M. Wu, X. Kang, Q. Wang, C. Zhou, C. Mohan, and A. Peng, “Regulator of G protein signaling-1 modulates paraquat-induced oxidative stress and longevity via the insulin like signaling pathway in *Caenorhabditis elegans*,” *Toxicol. Lett.*, vol. 273, pp. 97–105, May 2017.
- [22] P. ; Goos and A. N. Donev, “The D-Optimal Design of Blocked Experiments with Mixture Components,” 2006.
- [23] P. Goos and B. Jones, “Optimal Design of Experiments: A Case Study Approach - Peter Goos, Bradley Jones - Google Books,” *John Wiley & Sons, Ltd*, 2011. .
- [24] K. Apel and H. Hirt, “REACTIVE OXYGEN SPECIES: Metabolism, Oxidative Stress, and Signal Transduction,” *Annu. Rev. Plant Biol.*, vol. 55, no. 1, pp. 373–399, Jun. 2004.

- [25] L. A. Sena and N. S. Chandel, “Physiological roles of mitochondrial reactive oxygen species,” *Molecular Cell*, vol. 48, no. 2. Cell Press, pp. 158–167, 26-Oct-2012.
- [26] E. Gourgou and N. Chronis, “Chemically induced oxidative stress affects ASH neuronal function and behavior in *C. elegans*,” *Sci. Rep.*, vol. 6, no. 1, pp. 1–9, Dec. 2016.
- [27] E. H. Verbon, J. A. Post, and J. Boonstra, “The influence of reactive oxygen species on cell cycle progression in mammalian cells,” *Gene*, vol. 511, no. 1. Elsevier, pp. 1–6, 10-Dec-2012.
- [28] H. Chen *et al.*, “A review of toxicity induced by persistent organic pollutants (POPs) and endocrine-disrupting chemicals (EDCs) in the nematode *Caenorhabditis elegans*,” *Journal of Environmental Management*, vol. 237. Academic Press, pp. 519–525, 01-May-2019.
- [29] D. De *et al.*, “Visible light reduces *C. elegans* longevity.”
- [30] A. Rossi, K. Berger, H. Chen, D. Leslie, R. B. Mailman, and X. Huang, “Projection of the prevalence of Parkinson’s disease in the coming decades: Revisited,” *Mov. Disord.*, vol. 33, no. 1, pp. 156–159, Jan. 2018.
- [31] N. S. Caron, E. R. Dorsey, and M. R. Hayden, “Therapeutic approaches to huntington disease: From the bench to the clinic,” *Nature Reviews Drug Discovery*, vol. 17, no. 10. Nature Publishing Group, pp. 729–750, 01-Oct-2018.
- [32] E. Possik and A. Pause, “Measuring oxidative stress resistance of *caenorhabditis elegans* in 96-well microtiter plates,” *J. Vis. Exp.*, vol. 2015, no. 99, p. 52746, May 2015.
- [33] J. M. Van Raamsdonk and S. Hekimi, “Superoxide dismutase is dispensable for normal animal lifespan,” *Proc. Natl. Acad. Sci.*, vol. 109, no. 15, pp. 5785–5790, 2012.
- [34] K. Hasegawa, S. Miwa, K. Isomura, K. Tsutsumiuchi, H. Taniguchi, and J. Miwa, “Acrylamide-Responsive Genes in the Nematode *Caenorhabditis elegans*,” *Toxicol. Sci.*,

- vol. 101, no. 2, pp. 215–225, 2008.
- [35] S. Ahmad, “Oxidative stress from environmental pollutants,” *Arch. Insect Biochem. Physiol.*, vol. 29, no. 2, pp. 135–157, 1995.
- [36] Z. E. Suntres, “Role of antioxidants in paraquat toxicity,” *Toxicology*, vol. 180, no. 1, pp. 65–77, Oct. 2002.
- [37] R. J. Dinis-Oliveira, J. A. Duarte, A. Sánchez-Navarro, F. Remião, M. L. Bastos, and F. Carvalho, “Paraquat Poisonings: Mechanisms of Lung Toxicity, Clinical Features, and Treatment,” *Crit. Rev. Toxicol.*, vol. 38, no. 1, pp. 13–71, Jan. 2008.
- [38] N. Shome and S. Mukherji, “Application of kinetic bioluminescence inhibition assay using live cultures of *Aliivibrio fischeri* for determination of zinc toxicity,” *Int. J. Environ. Sci. Technol.*, vol. 15, no. 6, pp. 1313–1322, Jun. 2018.
- [39] P. . Babula *et al.*, “Simultaneous determination of 1, 4-naphthoquinone, lawsone, juglone and plumbagin by liquid chromatography with UV detection,” 2005.
- [40] Y. Kumagai, Y. Shinkai, T. Miura, and A. K. Cho, “The Chemical Biology of Naphthoquinones and Its Environmental Implications,” *Annu. Rev. Pharmacol. Toxicol.*, vol. 52, no. 1, pp. 221–247, Feb. 2012.
- [41] H. Fukui, M. Tsukada, H. Mizukami, and M. Tabata, “Formation of stereoisomeric mixtures of naphthoquinone derivatives in *Echium lycopsis* callus cultures,” *Phytochemistry*, vol. 22, no. 2, pp. 453–456, Jan. 1983.
- [42] J. Steinert, H. Khalaf, and M. Rimpler, “High-performance liquid chromatographic separation of some naturally occurring naphthoquinones and anthraquinones,” *J. Chromatogr. A*, vol. 723, no. 1, pp. 206–209, Feb. 1996.
- [43] A. Michaelakis, A. T. Strongilos, E. A. Bouzas, G. Koliopoulos, and E. A. Couladouros,

- “Larvicidal activity of naturally occurring naphthoquinones and derivatives against the West Nile virus vector *Culex pipiens*,” *Parasitol. Res.*, vol. 104, no. 3, pp. 657–662, Feb. 2009.
- [44] P. Seshadri, A. Rajaram, and R. Rajaram, “Plumbagin and juglone induce caspase-3-dependent apoptosis involving the mitochondria through ROS generation in human peripheral blood lymphocytes,” *Free Radic. Biol. Med.*, vol. 51, no. 11, pp. 2090–2107, Dec. 2011.
- [45] P. J. O’Brien, “Molecular mechanisms of quinone cytotoxicity,” *Chemico-Biological Interactions*, vol. 80, no. 1. Elsevier, pp. 1–41, 01-Jan-1991.
- [46] L. S. Hernández-Muñoz, M. Gómez, F. J. González, I. González, and C. Frontana, “Towards a molecular-level understanding of the reactivity differences for radical anions of juglone and plumbagin: An electrochemical and spectroelectrochemical approach,” *Org. Biomol. Chem.*, vol. 7, no. 9, pp. 1896–1903, May 2009.
- [47] L. Frézal and M. A. Félix, “*C. elegans* outside the Petri dish,” *Elife*, vol. 2015, no. 4, Mar. 2015.
- [48] R. N. Arey and C. T. Murphy, “Conserved regulators of cognitive aging: From worms to humans,” *Behav. Brain Res.*, vol. 322, pp. 299–310, Mar. 2017.
- [49] C. K. Leung, Y. Wang, S. Malany, A. Deonaraine, and K. Nguyen, “An Ultra High-Throughput, Whole-Animal Screen for Small Molecule Modulators of a Specific Genetic Pathway in *Caenorhabditis elegans*,” *PLoS One*, vol. 8, no. 4, p. 62166, 2013.
- [50] D. S. Portman, “Profiling *C. elegans* gene expression with DNA microarrays.,” *WormBook : the online review of C. elegans biology*. pp. 1–11, 2006.
- [51] O. Hobert and P. Loria, “Uses of GFP in *Caenorhabditis Elegans*,” in *Methods of*

- Biochemical Analysis*, vol. 47, John Wiley & Sons, Ltd, 2005, pp. 203–226.
- [52] R. Hunt-Newbury *et al.*, “High-Throughput In Vivo Analysis of Gene Expression in *Caenorhabditis elegans*,” *PLoS Biol.*, vol. 5, no. 9, p. e237, Sep. 2007.
- [53] V. Klaus *et al.*, “1,4-Naphthoquinones as inducers of oxidative damage and stress signaling in HaCaT human keratinocytes,” *Arch. Biochem. Biophys.*, vol. 496, no. 2, pp. 93–100, Apr. 2010.
- [54] T. K. Blackwell, M. J. Steinbaugh, J. M. Hourihan, C. Y. Ewald, and M. Isik, “SKN-1/Nrf, stress responses, and aging in *Caenorhabditis elegans*,” *Free Radical Biology and Medicine*, vol. 88, no. Part B. Elsevier Inc., pp. 290–301, 01-Nov-2015.
- [55] H. Inoue *et al.*, “The *C. elegans* p38 MAPK pathway regulates nuclear localization of the transcription factor SKN-1 in oxidative stress response,” *Genes Dev.*, vol. 19, no. 19, pp. 2278–2283, Oct. 2005.
- [56] K. P. Choe, A. J. Przybysz, and K. Strange, “The WD40 Repeat Protein WDR-23 Functions with the CUL4/DDB1 Ubiquitin Ligase To Regulate Nuclear Abundance and Activity of SKN-1 in *Caenorhabditis elegans*,” *Mol. Cell. Biol.*, vol. 29, no. 10, pp. 2704–2715, May 2009.
- [57] C. J. Kenyon, “The genetics of ageing,” *Nature*, vol. 464, no. 7288. Nature Publishing Group, pp. 504–512, 25-Mar-2010.
- [58] R. Voellmy and F. Boellmann, “Chaperone regulation of the heat shock protein response,” *Advances in Experimental Medicine and Biology*, vol. 594. Springer New York, pp. 89–99, 2007.
- [59] N. A. Bishop and L. Guarente, “Two neurons mediate diet-restriction-induced longevity in *C. elegans*,” *Nature*, vol. 447, no. 7144, pp. 545–549, May 2007.

- [60] T. Gidalevitz, V. Prahlad, and R. I. Morimoto, “The stress of protein misfolding: From single cells to multicellular organisms,” *Cold Spring Harb. Perspect. Biol.*, vol. 3, no. 6, pp. 1–18, Jun. 2011.
- [61] J. H. An and T. K. Blackwell, “Specification To a Conserved Oxidative Stress Response,” *Genes Dev.*, vol. 17, no. 15, pp. 1882–1893, 2003.
- [62] T. A. Crombie, L. Tang, K. P. Choe, and D. Julian, “Inhibition of the oxidative stress response by heat stress in *Caenorhabditis elegans*,” 2016.
- [63] A. Benedetto *et al.*, “New label-free automated survival assays reveal unexpected stress resistance patterns during *C. elegans* aging,” *Aging Cell*, Jul. 2019.
- [64] J. M. A. Tullet, “DAF-16 target identification in *C. elegans*: past, present and future,” *Biogerontology*, vol. 16, no. 2. Kluwer Academic Publishers, pp. 221–234, 2015.
- [65] J. R. Cypser, D. Kitzenberg, and S. K. Park, “Dietary restriction in *C. elegans*: Recent advances,” *Exp. Gerontol.*, vol. 48, no. 10, pp. 1014–1017, Oct. 2013.
- [66] J. M. A. Tullet *et al.*, “Direct Inhibition of the Longevity-Promoting Factor SKN-1 by Insulin-like Signaling in *C. elegans*,” *Cell*, vol. 132, no. 6, pp. 1025–1038, Mar. 2008.
- [67] T. Okuyama *et al.*, “The ERK-MAPK Pathway Regulates Longevity through SKN-1 and Insulin-like Signaling in *Caenorhabditis elegans* \* □ S Downloaded from,” *J. Biol. Chem.*, vol. 285, no. 39, pp. 30274–30281, 2010.
- [68] W. N. Tawe, M. L. Eschbach, R. D. Walter, and K. Henkle-Dührsen, “Identification of stress-responsive genes in *Caenorhabditis elegans* using RT-PCR differential display,” *Nucleic Acids Res.*, vol. 26, no. 7, pp. 1621–1627, Apr. 1998.
- [69] C. D. Link and C. J. Johnson, “Reporter transgenes for study of oxidant stress in *Caenorhabditis elegans*,” in *Methods in Enzymology*, vol. 353, Academic Press Inc., 2002,

- pp. 497–505.
- [70] B. Leiers, A. Kampkötter, C. G. Grevelding, C. D. Link, T. E. Johnson, and K. Henkle-Dührsen, “Original Contribution A STRESS-RESPONSIVE GLUTATHIONE S-TRANSFERASE CONFERS RESISTANCE TO OXIDATIVE STRESS IN CAENORHABDITIS ELEGANS,” 2003.
- [71] S. Robida-Stubbs *et al.*, “TOR signaling and rapamycin influence longevity by regulating SKN-1/Nrf and DAF-16/FoxO,” *Cell Metab.*, vol. 15, no. 5, pp. 713–724, May 2012.
- [72] B. Onken and M. Driscoll, “Metformin Induces a Dietary Restriction–Like State and the Oxidative Stress Response to Extend *C. elegans* Healthspan via AMPK, LKB1, and SKN-1,” *PLoS One*, vol. 5, no. 1, p. e8758, Jan. 2010.
- [73] J. A. Rollins, D. Shaffer, S. S. Snow, P. Kapahi, and A. N. Rogers, “Dietary restriction induces posttranscriptional regulation of longevity genes,” *Life Sci. Alliance*, vol. 2, no. 4, 2019.
- [74] B. Jones and P. Goos, “D-optimal design of split-split-plot experiments,” *Biometrika*, vol. 96, no. 1, pp. 67–82, Mar. 2009.
- [75] D. Lucio *et al.*, “Optimization and evaluation of zein nanoparticles to improve the oral delivery of glibenclamide. In vivo study using *C. elegans*,” *Eur. J. Pharm. Biopharm.*, vol. 121, pp. 104–112, Dec. 2017.
- [76] M. C. Letizia, M. Cornaglia, G. Tranchida, R. Trouillon, and M. A. M. Gijs, “A design of experiment approach for efficient multi-parametric drug testing using a *Caenorhabditis elegans* model,” *Integr. Biol. (United Kingdom)*, vol. 10, no. 1, pp. 48–56, Jan. 2018.
- [77] R. K. Meyer and C. J. Nachtsheim, “The coordinate-exchange algorithm for constructing exact optimal experimental designs,” *Technometrics*, vol. 37, no. 1, pp. 60–69, 1995.

- [78] T. Stiernagle, “Maintenance of *C. elegans* \*.”
- [79] F. R. G. Amrit, R. Ratnappan, S. A. Keith, and A. Ghazi, “The *C. elegans* lifespan assay toolkit,” *Methods*, vol. 68, no. 3, pp. 465–475, Aug. 2014.
- [80] M. Senchuk, D. Dues, and J. Van Raamsdonk, “Measuring Oxidative Stress in *Caenorhabditis elegans*: Paraquat and Juglone Sensitivity Assays,” *Bio-Protocol*, vol. 7, no. 1, pp. 1–16, 2017.
- [81] P. R. Hunt, T. G. Son, M. A. Wilson, Q.-S. Yu, and W. H. Wood, “Extension of Lifespan in *C. elegans* by Naphthoquinones That Act through Stress Hormesis Mechanisms,” *PLoS One*, vol. 6, no. 7, p. 21922, 2011.
- [82] N. Bhatla and H. R. Horvitz, “Light and Hydrogen Peroxide Inhibit *C. elegans* Feeding through Gustatory Receptor Orthologs and Pharyngeal Neurons,” *Neuron*, vol. 85, no. 4, pp. 804–818, Feb. 2015.
- [83] J. Paek *et al.*, “Mitochondrial SKN-1/Nrf mediates a conserved starvation response,” *Cell Metab.*, vol. 16, no. 4, pp. 526–537, Oct. 2012.
- [84] M. Åkerfelt, R. I. Morimoto, and L. Sistonen, “Heat shock factors: Integrators of cell stress, development and lifespan,” *Nature Reviews Molecular Cell Biology*, vol. 11, no. 8. Nature Publishing Group, pp. 545–555, 14-Aug-2010.
- [85] S. N. Politis, P. Colombo, G. Colombo, and D. M. Rekkas, “Design of experiments (DoE) in pharmaceutical development,” *Drug Development and Industrial Pharmacy*, vol. 43, no. 6. Taylor and Francis Ltd., pp. 889–901, 03-Jun-2017.
- [86] S. Kowalski, J. A. Cornell, and G. G. Vining, “A new model and class of designs for mixture experiments with process variables,” *Commun. Stat. - Theory Methods*, vol. 29, no. 9–10, pp. 2255–2280, 2000.

- [87] G. Wrobel, J. Schlingemann, L. Hummerich, H. Kramer, P. Lichter, and M. Hahn, “Optimization of high-density cDNA-microarray protocols by ‘design of experiments’ .,” *Nucleic Acids Res.*, vol. 31, no. 12, pp. e67–e67, Jun. 2003.
- [88] D. Midkiff and A. San-Miguel, “Microfluidic technologies for high throughput screening through sorting and on-chip culture of *C. elegans*,” *Molecules*, vol. 24, no. 23. MDPI AG, p. 4292, 25-Nov-2019.
- [89] A. San-Miguel *et al.*, “Deep phenotyping unveils hidden traits and genetic relations in subtle mutants,” *Nat. Commun.*, vol. 7, pp. 1–13, 2016.
- [90] S. Saberi-Bosari, J. Huayta, and A. San-Miguel, “A microfluidic platform for lifelong high-resolution and high throughput imaging of subtle aging phenotypes in *C. elegans*,” *Lab Chip*, vol. 18, no. 20, pp. 3090–3100, 2018.
- [91] M. M. Crane, K. Chung, J. Stirman, and H. Lu, “Microfluidics-enabled phenotyping, imaging, and screening of multicellular organisms,” *Lab on a Chip*, vol. 10, no. 12. Royal Society of Chemistry, pp. 1509–1517, 01-Jun-2010.